Rapid turnover of sex chromosomes is associated with speciation in Neotropical armored catfish *Harttia* (Siluriformes, Loricariidae)

Francisco de M. C. Sassi[1, 2, 3], Fernando Henrique S. de Souza[2, 4], Manolo F. Perez[5], Foyez Shams[3], Tariq Ezaz[3], Geize A. Deon[2, 3], Thomas Liehr[6]*, Luohao Xu[1], Marcelo de B. Cioffi[2]

[1] MOE Key Laboratory of Freshwater Fish Reproduction and Development, College of Life Sciences, Southwest University, Chongqing 400715, China.
[2] Laboratory of Evolutionary Cytogenetics, Universidade Federal de São Carlos, São Carlos – SP 13565-905, Brazil.
[3] Institute for Applied Ecology, University of Canberra, Canberra – ACT 2617, Australia.
[4] Department of Zoology, Faculty of Science, Charles University, Prague 12800, Czech Republic.
[5] Real Jardín Botánico – RJB-CSIC, Madrid 28014, Spain.
[6] Institut für Humangenetik, Universitätsklinikum Jena, 07747 Jena, Germany

These authors jointly supervised this work: Luohao Xu, Marcelo de B. Cioffi.

***Corresponding author:** thomas.liehr@med-uni.jena.de

Abstract

The genus *Harttia* represents an important repository of multiple sex chromosomes, as they are found in more than a quarter of its valid species with distinct degrees of heteromorphism. We demonstrate that the recent and independent emergence of two distinct multiple sex chromosome systems (X_1X_2Y and XY_1Y_2) is associated with accelerated speciation rates. Using DArTseq data from 17 *Harttia* species, we investigate the sex chromosomes evolution and potential role in diversification. A time-calibrated phylogeny revealed main divergences occurring from 6 to 10 Mya, coinciding with Amazon River formation and other core river capture events in South America. Reconstruction of ancestral states (areas and chromosome number), combined with the identification of sex-linked markers, suggests the ancestor carried a karyotype of 2n=58 and homomorphic XY, occupying either the South and Southeast Atlantic drainages or the Eastern Amazon. These findings underscore the potential contribution of multiple sex chromosomes and turnovers in accelerating speciation.

Keywords: SNP, phylogenetics, DArT-seq, sex-linked markers, probabilistic modeling

1. Introduction

In the canonical model of sex chromosome evolution, the emergence of a sex-determining gene is followed by the suppression of recombination around this locus, allowing the accumulation of sexually antagonistic alleles and other sex-linked sequences[1,2]. Structural rearrangements of chromosomes, such as inversions, might further consolidate this recombination suppression, resulting in the gradual differentiation and heteromorphy of the sex chromosomes[3]. Nonetheless, before these chromosome rearrangements in regions where recombination persists, such as the pseudoautosomal region (PAR), sex-linked loci may still recombine between the X and Y or Z and W chromosomes[4]. These dynamics are particularly relevant in species exhibiting homomorphic sex chromosomes, where recombination

suppression may be either partial or recent[5]. Comprehending the inheritance patterns, chromosomal locations, and evolutionary trajectories of sex-linked markers is crucial for elucidating the origins and diversity of sex-determination systems[4,6].

Multiple sex chromosome systems originate from chromosomal rearrangements that occur in simple systems (XX/XY or ZZ/ZW). These rearrangements may involve fissions of ancestral chromosome pairs or fusions with autosomes and are generally considered rare in eukaryotes[7–10], found in only about 100 fish species[11]. However, our understanding of the evolution of sex chromosomes remains largely shaped by studies conducted in a limited number of model organisms, which typically possess heteromorphic sex chromosomes at advanced evolutionary stages, thus providing a restricted view of the diversity and complexity of sex determination systems found in nature[4].

In this context, the Neotropical armored catfish *Harttia* (Siluriformes: Loricariidae) is emerging as an exceptional model system to study multiple sex chromosomes with distinct degrees of degeneration. Comprising 28 valid species[12], this monophyletic genus[13,14] is distributed across rheophilic habitats of the Brazilian and Guiana Shields. *Harttia* exhibits the highest number of multiple sex chromosome systems among fish, with about 28% of species displaying heteromorphic sex chromosomes[15], a proportion matched only by *Notobranchius* killifishes[15–17]. These systems vary in complexity and differentiation, making *Harttia* a unique model for studying repeated sex chromosome turnover and the independent origins of multiple sex chromosome systems. Conventional and molecular cytogenetic data revealed an exceptional diversity of 2n (from 52 to 62 chromosomes) and two independent male-heterogametic systems (Figure 1): the XX/XY_1Y_2 and its homologous XX/XY in species from South and Southeast Brazil, and the $X_1X_1X_2X_2/X_1X_2Y$ system with a corresponding XX/XY in Amazonian species[18–21]. The rare XX/XY_1Y_2 system, described for only nine fish species to date[21], is found in three *Harttia* species: *H. carvalhoi* and *Harttia* sp. 1, originating from a sex chromosome-autosome translocation (SC-A) involving an ancestral XX/XY configuration (seen in *H. torrenticola*), with a subsequent reciprocal translocation with an additional autosomal pair giving rise to the XX/XY_1Y_2 seen in *H. intermontana*[18,21–23]. Conversely, in the Amazonian lineage, a fission of the ancestral XY system (likely the same seen in *H. rondoni*) is proposed to have led to the emergence of the X_1X_2Y system found in *H. duriventris*, *H. villasboas*, and *H. punctata*[24]. Comparative analyses of satellite DNA content further reveal distinct degrees of differentiation among these systems, suggesting multiple independent origins and divergent evolutionary trajectories[25,26].

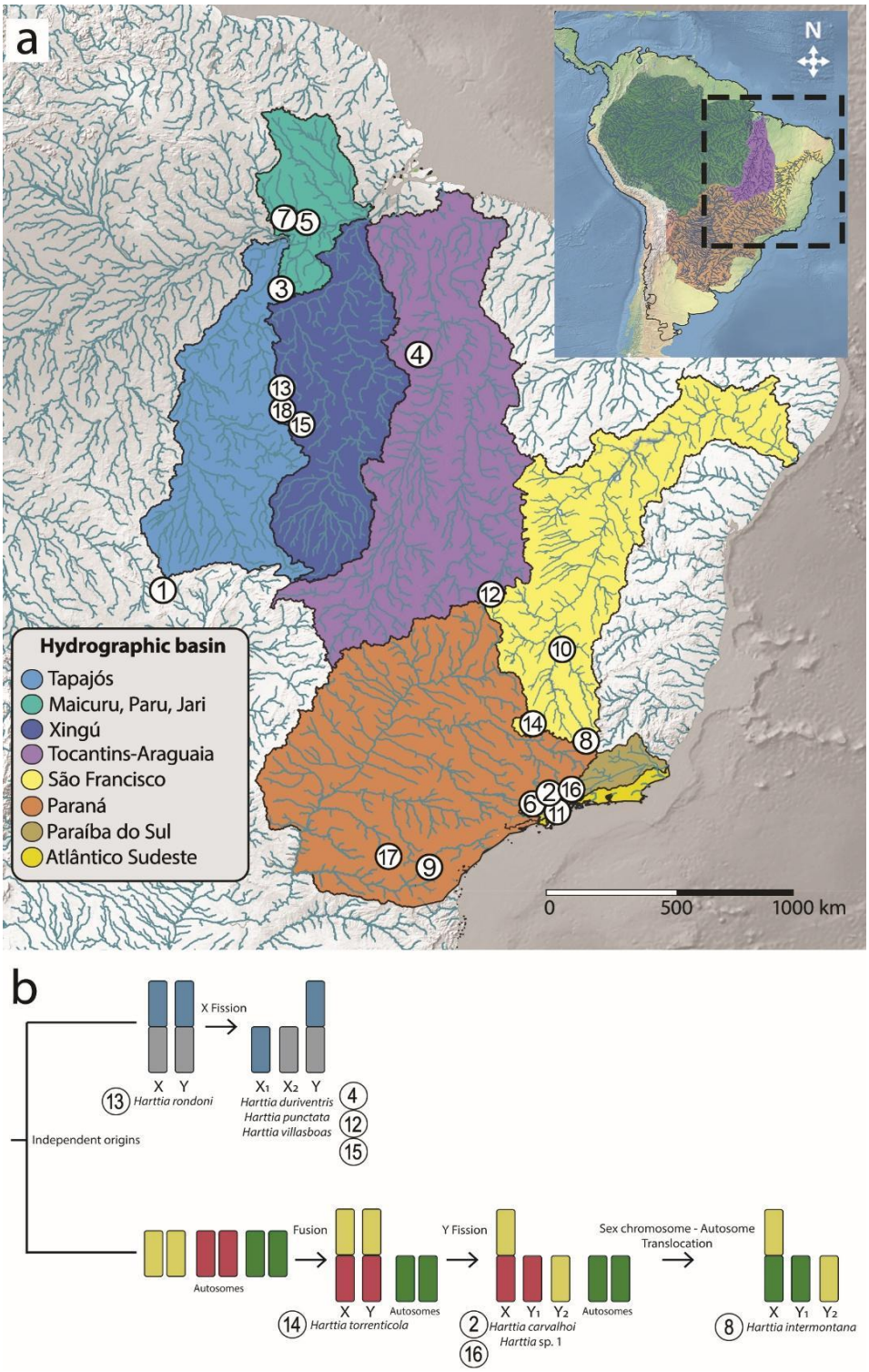

Figure 1. Geographical distribution and sex chromosome evolution pathways of the investigated species. a) Partial Brazilian map indicating sample sites (circles) and river basins (colored areas). Numbering follows Supplementary Table 1**.** The upper right corner map shows the Neotropical region (black contour line), and the four main basins: Amazon (dark green), Tocantins-Araguaia (purple), La Plata (orange), and São Francisco (yellow). **b)** Schematic view of the proposed evolutionary pathways of *Harttia* sex chromosomes, based on previous cytogenetic data[18–28].

Without the availability of a reference genome, complexity reduction techniques have proven to be powerful tools for genomic research in non-model organisms[29–31]. These approaches offer a cost-effective means of generating thousands of molecular markers, suitable for investigating genetic polymorphisms, assessing population structure, and exploring patterns of genome evolution[32]. Analyses using large nuclear marker datasets provide higher resolution and assist in overcoming issues such as incomplete lineage sorting and restricted taxon sampling[33,34]. DArTseq (Diversity Arrays Technology sequencing)[35] has emerged as a widely used method due to its ability to target low-copy and predominantly active genomic regions, which may include sex-specific loci, before high-throughput sequencing[36]. These features have enabled DArTseq applications in a broad range of taxa and research areas, including genetic diversity, hybridization, admixture, phylogeography, phylogenetics, and the identification of sex-linked markers[37–42]. Sex-linked markers provide key insights into the localization and structure of sex-determining regions, offering a molecular entry point into the evolutionary processes that shape sex chromosome systems[37].

In this current study, we performed DArTseq in 17 *Harttia* species and one outgroup species (*Farlowella* sp.) to examine the genomic architecture of sex chromosome evolution in this dynamic genus (Supplementary Table 1). Our primary objective was to identify the likely mechanisms underlying the diversity of multiple sex chromosomes in the genus. To this end, we focused on identifying putative sex-linked markers and analyzing their distribution across species with different sex chromosome systems. A comprehensive phylogenetic tree based on SNP data was constructed, integrating spatial and cytogenetic information by reconstructing ancestral distribution areas and modeling chromosome number evolution using probabilistic approaches. Our findings indicate that the rapid turnover of multiple sex chromosome systems, originating from an ancestral XY configuration, may be linked to an accelerated tempo of diversification in *Harttia.*

2. Results

2.1 Evolutionary relationships in Harttia

A total of 95,305 SNPs and 282,275 SilicoDArT (presence and absence) loci were generated for 107 individuals from 17 *Harttia* and one *Farlowella* species. The resulting phylogeny, constructed using 24,858 SNP markers after stringent filtering, grouped all *Harttia* species into three primary clades, each exhibiting strong geographic coherence (Figure 2a). Exceptionally, *Harttia* sp. 2 was placed as a single ancestral branch to all remaining *Harttia*, not included in any of the three clades. Clade I comprises species from the Guiana Shield drainages (*H. fowleri* and *H. guianensis*). At the same time, Clade II included species from Amazon Brazilian Shield drainages, specifically the Xingu, Tapajós, and Tocantins-Araguaia River Basins (*H. duriventris*, *H. dissidens*, *H. punctata*, *H. rondoni*, *H. villasboas*, and *Harttia* sp. 3); and Clade III contained species distributed across Southeastern and South Atlantic drainages and from the La Plata basin (*H. carvalhoi*, *H. torrenticola*, *H. intermontana*, *H. longipinna*, *H. gracilis*, *H. loricariformis*, *H. kronei*, and *Harttia* sp. 1) (Figure 2a). The divergence between *Harttia* and *Farlowella* was estimated at ~29.5 million years ago (Mya), with Clade I split about 10 Mya and the divergence between Clades II and III taking place at ~7.9 Mya. The origin of multiple sex chromosome systems was inferred at 5.8 Mya for Clade II (X_1X_2Y system, based on the splitting of *H. punctata*) and at 1.3 Mya for Clade III (XY_1Y_2 system, based on the splitting of *H. intermontana*). The Principal Component Analysis (PCA) of autosomal SNPs (PC1 = 28.5%, PC2 = 18.9%) identified five distinct clusters aligned with phylogenetic clades and geographic distributions (Supplementary Figure 2), categorizing *Harttia* species into three primary clusters, while *Harttia* sp. 2 and the outgroup *Farlowella* sp. constituted separate groups. The complete phylogeny with all individuals is presented in Supplementary Figure 1, and complete mean time-calibration estimates are provided in Supplementary Table 2.

Examining the number of lineages over time reveals two significant shifts (Figure 2b, arrows). These shifts overlap with splitting times that are mostly related to clades with the presence of multiple sex chromosomes, at 2.5 Mya and 1.3 Mya (i.e., the first for the clade composed of *Harttia* sp. 3, *H. duriventris*, *H. rondoni* and *H. villasboas*, and the second for the clade *H. intermontana*, *H. torrenticola, H. carvalhoi*, and *Harttia* sp. 1 (Figure 2a,b). Indeed, state-dependent diversification analyses with the Binary State Speciation and Extinction model (BiSSE) revealed substantial differences in speciation rates associated with the presence or absence of multiple sex chromosomes. Lineages with simple sex chromosomes (state 0) exhibited a markedly lower speciation rate (λ_0 = 0.032, CI95% = 0.026-0.290) than those with multiple sex chromosomes (state 1; λ_1 = 0.941, CI95% = 0.485-3.064). The turnover rate for state 0 (ε = 1.040, CI95% = 0.776-1.230), calculated as the ratio between extinction and speciation, suggests that extinction is approximately equal to speciation in this group.

Additionally, the estimated transition rate ($q_{0 \leftrightarrow 1}$) from the absence to the presence of multiple sex chromosomes indicates a moderate probability of trait evolution over time (0.375, CI95% = 0.202-1.530). These modeling results suggest a strong association between the presence of multiple sex chromosomes and increased diversification rates in *Harttia* (p-value = 0.005) (Figure 2c, Table 1).

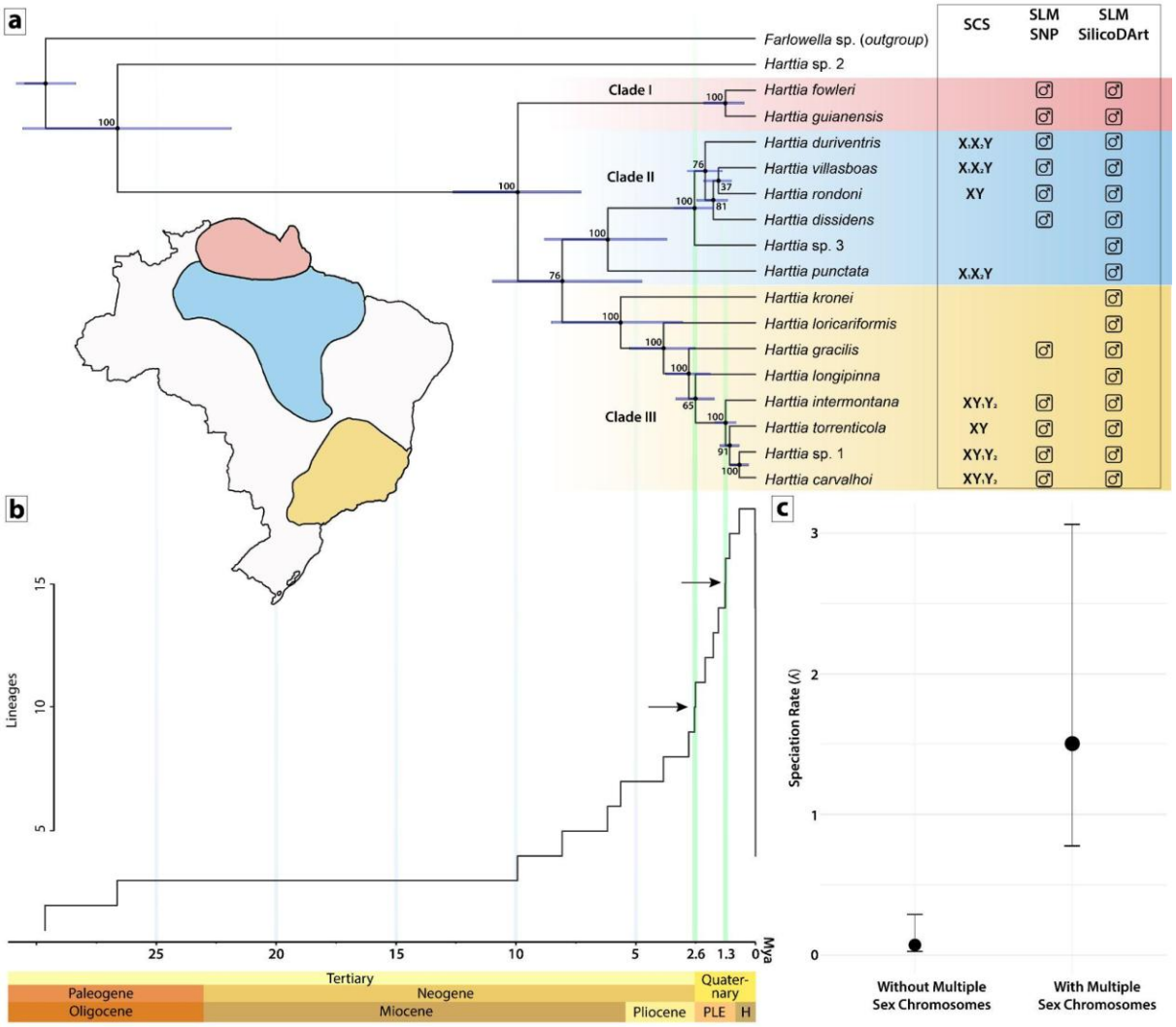

Figure 2. **Evolutionary relationships in *Harttia* and the potential role of multiple sex chromosomes in accelerating speciation rates**. **a)** Time-calibrated maximum likelihood phylogenetic relationships of *Harttia* species, using *Farlowella* sp. as an outgroup, recovered from 1,381 autosomal SNPs per species (24,858 SNP markers in total) generated by DArTSeq from 108 individuals. Clade colors correspond to their distribution indicated in the map. Cytogenetically described sex chromosome systems are indicated (SCS). Sex-linked markers, either SNPs or SilicoDArT are presented using the male symbol to indicate male-heterogamety (XY). Node bars correspond to the 95% HPD interval of divergence times and values at nodes indicate bootstrap support. **b)** Lineage through time plot, with arrows indicating major shifts in

169 the number of lineages at 2.6 and 1.3 Mya, accompanied by green lines indicating their
170 coincidence with the rapid diversification of clades with multiple sex chromosomes in the
171 phylogeny. Time scale is the same for both the phylogeny and the lineage through time plot.
172 PLE stands for Pleistocene and H for Holocene. **c)** Speciation rates in clades without and with
173 multiple sex chromosomes inferred by BiSSE. The dots represent the main estimation, and the
174 lines are the 95% confidence intervals.
175
176 **Table 1.** Parameter estimates from the BiSSE model evaluating the association between the
177 presence of multiple sex chromosomes and diversification rates. Speciation rates (λ) are
178 reported separately for lineages without (state 0) and with (state 1) multiple sex chromosomes.
179 Turnover rate (ε) corresponds to the extinction/speciation ratio for state 0. The transition rate
180 ($q_{0\rightarrow1}$) reflects the rate of evolution from the absence to the presence of multiple sex
181 chromosomes. Estimates are presented alongside their 95% confidence intervals.

Parameter	Estimate	95% CI
Speciation in clades without multiple sex chromosomes (λ_0)	0.032	0.016 – 0.141
Speciation in clades with multiple sex chromosomes (λ_0)	0.941	0.485 – 1.947
Turnover (ε_0)	1.040	0.858 – 1.243
Transition rate ($q_{0\rightarrow1}$)	0.248	0.135 – 0.811

182
183 ***2.2 Sex-linked markers***
184 The application of a Bonferroni correction for multiple testing across the 95,305 SNP
185 markers generated from the sequencing plate resulted in a stringent per-test significance
186 threshold ($P_corrected \approx 2.62 \times 10^{-6}$). This low threshold indicates that the identified sex-linked
187 SNPs are highly unlikely to be false positives arising from random assortment. We focused the
188 false discovery rate calculation on the SNP data due to its co-dominant nature, which provides
189 higher confidence in genotyping calls for assessing sex-linked patterns rather than dominant
190 SilicoDArT markers. Nevertheless, we acknowledge the intrinsic limitations of our sample size
191 (n=3 per sex) and recognize that a greater sampling is required to provide better statistical
192 confidence for the SLM.
193 Across all samples, we identified 443 candidates of sex-linked markers: 95 XY and 16
194 ZW markers from the SNPs dataset and 316 XY and 16 ZW markers from the SilicoDArT
195 dataset (Figure 3a; Supplementary Data 1 and 2 available at

https://github.com/sassichico/harttia). PCA of the sex-linked SNPs (Supplementary Figure 2) revealed three main clusters: one composed solely of *H. intermontana*, a second grouping *H. carvalhoi*, *Harttia* sp. 1, and *H. torrenticola*, and a third containing the remaining species, with a minor subcluster of *H. gracilis*. Using a 100% similarity threshold, we identified three shared sex-linked SNPs and 33 shared SilicoDArT markers (Supplementary Table 3). Shared sex-linked markers were detected in two groups: i) *H. carvalhoi* and *H. intermontana* (XY_1Y_2 system) and ii) a subset of species within Clade II, all in both groups corresponding to XY SLM. Those shared SLMs were only identified inside the groups and not between them, suggesting independent origins of those systems. As an additional step to verify the trustability of the sex-linked markers, since *Harttia* species lack assembled genomes, we cross-mapped the herein obtained SLM in the single Loricariidae chromosome-level genome available at NCBI (*Pterygoplichthys pardalis* ASM5023128v1). Although this genome lacks an identification of sex chromosomes[43], we obtained large homologous clusters in chromosomes 2 and 3, suggesting that those SLMs might be not only valid for *Harttia* but also for other loricariids and reinforcing the independent origin of both multiple systems in *Harttia* (Figure 3b).

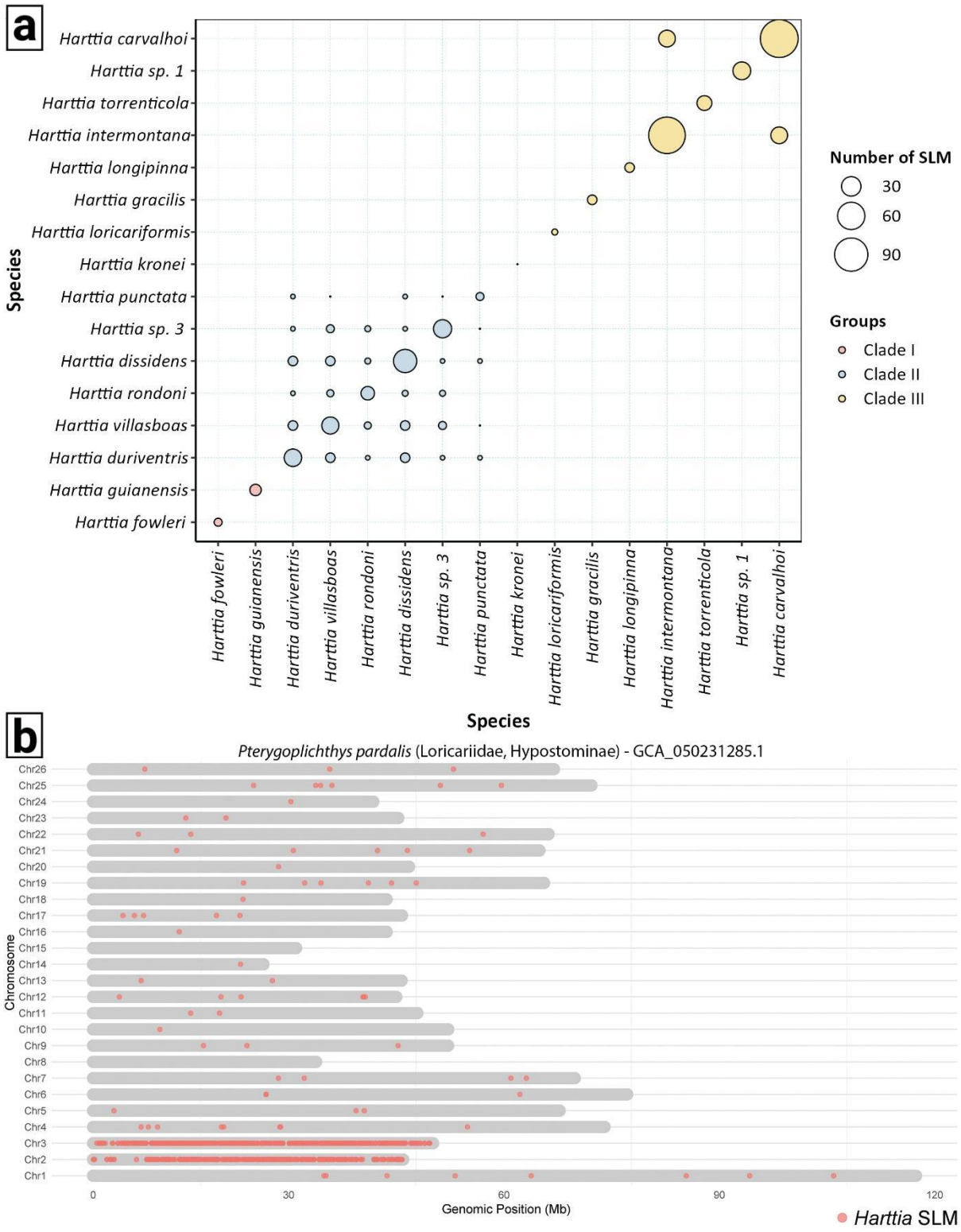

Figure 3. **Independent evolution of sex chromosomes in *Harttia* underscored from sex-linked markers**. **a)** Bubble plot showing the number of sex-linked markers per species, colored according to the clade they belong to, as shown in Figure 2. The off-diagonal bubbles represent overlapped sex-linked markers, with the size of the bubble representing the number of these shared SLMs. **b)** Cross-mapping of *Harttia* sex-linked markers in the chromosome-level genome of *Pterygoplichthys pardalis* (Loricariidae, Hypostominae).

220 ***2.3 Biogeographical modeling and ancestral karyotype***

221 A key objective of this study was to infer the historical processes underlying the current
222 distribution and diversity of *Harttia*. We therefore employed biogeographical modeling to
223 estimate ancestral ranges and identify potential dispersal routes, coupled with ancestral
224 chromosome number reconstruction to trace the role of chromosome evolution in speciation.
225 Resolving these questions is fundamental to testing hypotheses about the drivers of diversity
226 in this widely distributed genus. The DIVALIKE model was selected as the best-fitting model
227 based on AICc scores (Table 2, Figure 4a). Although likelihood scores between the DEC and
228 DIVALIKE models showed minimal variation, the estimated ancestral ranges diverged notably
229 after the 23 Mya time slice (see Supplementary Figure 3 for DEC estimates). ΔAIC values
230 indicated only a marginal improvement for DIVALIKE over DEC, the same occurring for Akaike
231 weights (W_i), indicating a little uncertainty between them. Both models converged on similar
232 ancestral area reconstructions after the 10 Mya threshold. The most inclusive *Harttia* clade
233 was inferred to have occupied either the Southern or Southeastern Atlantic drainages (A). The
234 most recent common ancestor of Clade III was likely restricted to the "A", whereas Clade II
235 appears to have been confined to the Amazon Brazilian Shield (B). DIVALike suggested an
236 ancestral distribution along the "A" for the whole *Harttia* clade, with the ancestor of *Harttia* and
237 *Farlowella* likely ranging either on the "A" or "B".

238

239 **Table 2.** Models implemented in BioGeoBEARS with their respective Log-likelihood (lnL),
240 dispersal (d), and extinction (e) parameters, corrected Akaike information criterion (AICc),
241 difference in AICc values compared to the best-fit model (ΔAIC), and Akaike weights (W_i).

Model	lnL	*d*	*e*	AICc	ΔAIC	Weight (W_i)
DEC	-39.28528	0.0268696	0.0304716	82.59056	0.97624	0.38
DIVALike	-38.80716	0.02924266	0.02305116	81.61432	0	0.62
BayAreaLike	-45.32449	0.03725671	0.08521665	94.64898	13.03466	0.0009

242

243 The ancestral 2n found at the root of the phylogeny proposed by the model Dys was
244 2n = 62, indicating that events of descending dysploidy (chromosome fusions) were
245 predominant throughout *Harttia* chromosomal evolution. For the *Harttia* clade (excluding
246 *Farlowella*), the same ancestral 2n was found. In clade III, the ancestral diploid number for
247 species exhibiting cytogenetically identifiable sex chromosomes (*H. intermontana*, *H.*
248 *torrenticola*, *H. carvalhoi*, and *Harttia* sp. 1) is 2n = 56, while in clade II (the most
249 comprehensive clade, including *H. punctata*, *H. duriventris,* and *H. villasboas*), it is 2n = 58
250 (Figure 4b, Supplementary Data 3 available at https://github.com/sassichico/harttia).

251

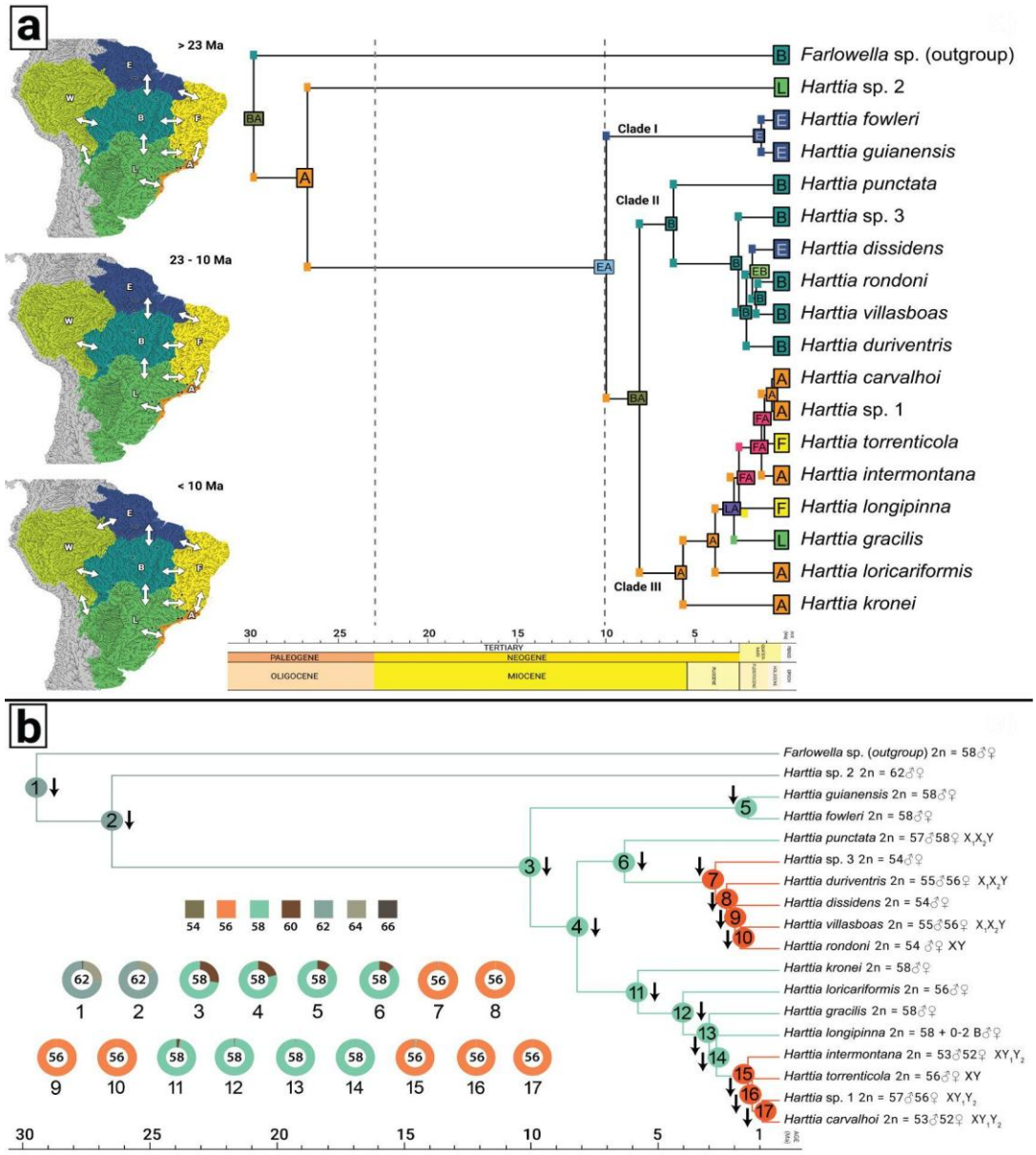

Figure 4. Biogeographic and karyotype modeling for the ancestral characters of *Harttia*. a) Ancestral range of *Harttia* estimated from the best model DIVALike in BioGeoBEARS. Dashed lines correspond to the three time slices defined for modeling: > 23 Mya, 23-10 Mya, and < 10 Mya, which are also represented in the maps with the connections allowed at each (white arrows). The color and letters of tips in phylogeny correspond to the same color in the map on the left, representing the biogeographical areas. At the nodes, the letters represent the sum of the areas of the tips, colored by a mean color of those. **b)** The evolution of diploid numbers in *Harttia* was inferred in ChromEvol v2.0 with the Dys model. Each branch is colored with the same color indicated in the legend for its respective ancestral 2n. Pie charts indicate the probability of the ancestral 2n recovered for each node, indicated by numbers (1-17) in the nodes of the phylogenetic tree. The diploid number and sex chromosome system of the

species are shown after their names. Chromosome loss events (down arrows) were predominant (**Supplementary Data 3**).

3. Discussion

Our study suggests that the diversification of *Harttia* is likely driven by a combination of biogeographical events, karyotype restructuring, and multiple independent origins of sex chromosome systems. Our phylogenetic reconstruction suggests that *Harttia* diversification occurred primarily over the past 10 million years, coinciding with major geological and hydrological changes in South America. Notably, the emergence of multiple sex chromosome systems occurred during ~5.6 and ~1.2 Mya are associated with accelerated speciation rates, as indicated by BiSSE modeling, suggesting an important role of those systems in the evolution and speciation of the genus. These findings reshape our understanding of the genus and present *Harttia* as a model for studying rapid and recurrent sex chromosome turnover and its role in speciation.

The nuclear-based phylogeny based on 1,381 SNPs per species (24,858 SNP markers in total) resolves three major *Harttia* clades but differs from previous mitochondrial and morphological studies. While broadly consistent with earlier studies[13,14], our topology reveals key discrepancies such as the placement of *H. fowleri* within clade I instead of clade II. The distribution of *H. fowleri* suggests a complex pattern with most registers from Mahury River (French Guyana) and few in drainages from the left bank of the Amazon River in Brazil (e.g. Maicuru River - our sampling site). This region in North Brazil harbors rivers that drain from the Guiana Shield and is a recognized region with poor knowledge on the ichthyofauna[44–46]. A similar pattern of distribution also occur for the species *H. guianensis*, which is also placed in the clade I. Notably, *Harttia* species are usually restricted to small stretches of rivers with rocky or sandy-bottom and fast flowing waters[47] and the Amazon River might serve as a great biogeographical barrier for species for clade I and II + III (Figure 2), as widely recognized for several terrestrial and aquatic species[48–50].

A distinct sister-group relationship involving *H. dissidens*, indicating more complex interspecific relationships than previously recognized. In our phylogeny, *H. dissidens* is sister to the *H. rondoni* + *H. villasboas* clade, with this group forming a sister lineage to the *H. duriventris*, and all these species sister to *H. punctata*, the earliest diverging species in clade II at ~6 mya. In contrast, Londoño-Burbano and Reis[14] recovered *H. dissidens* as more ancestral to the whole clade II, while in Covain et al.[13], *H. dissidens* was placed as a sister to most species, with only *H. punctata* showing an older diversification. Besides, *Harttia* sp. 2 was recovered herein as deeply divergent from the remaining *Harttia* species, with an estimated split occurring ~25 Mya. This lineage exhibits a distinct karyotype, which is highly similar to that reported in *H. absaberi*[51], with 2n = 62 chromosomes and a high number of

301 interstitial telomeric sites (ITS)[21]. SLMs are found in all *Harttia* species but *Harttia* sp. 2,
302 supporting a distinction of the latter from the remaining *Harttia* species (Figure 3). Indeed, *H.*
303 *absaberi* was included in the molecular and morphological phylogeny presented by
304 Cherobim[52], who recovered it as more closely related to other Loricariinae genera than to
305 *Harttia*, suggesting it may warrant placement in a separate genus. Although our sampling
306 included only a single outgroup (*Farlowella*), which diverged from *Harttia* ~30 Mya, the
307 combined evidence from phylogenetic distance, divergence time, and cytogenetic data
308 therefore supports the hypothesis that *Harttia* sp. 2, like *H. absaberi*, may not belong to *Harttia*
309 sensu stricto.

310 Biogeographically, *Harttia* diversification mirrors Neotropical River evolution (Figure
311 4a). The divergence of major clades aligns with the Miocene uplift of the Andes Mountain range
312 that led to the reconfiguration of most drainage systems in South America, especially in the
313 Amazonian region. The distribution of clade II species across formerly interconnected basins
314 (e.g., Tocantins-Araguaia, Xingu, Tapajós) reflects historical dispersal followed by vicariant
315 speciation, a pattern corroborated by similar trends in other loricariid taxa and the highly similar
316 ichthyofauna of those basins, as reported previously in other lineages such as *Cynolebias* spp.,
317 *Centromochlus schultzi*, and several Prochilodontidae[53–57]. Indeed, the redirection of river
318 courses occurred in the late Miocene, especially proto-Tapajós, proto-Xingu, and proto-
319 Tocantins-Araguaia[54], the development of mega-wetlands, and the formation of interfluves
320 such as the Purus Arch and the Serra do Cachimbo introduced new opportunities for both
321 dispersal and vicariant isolation among freshwater organisms, particularly loricariids[58], which
322 agrees with the patterns here observed for *Harttia*. Notably, patterns of biogeographical
323 diversification seen in clade III coincide with the time when the uplift of the Serra do Mar and
324 Serra da Mantiqueira Mountain ranges occurred. These events have isolated certain portions
325 of the La Plata Basin from the Atlantic South and Southeastern Drainages, so as from the São
326 Francisco River Basin[58,59], leading to vicariant processes among their similar ichthyofauna, as
327 also observed for *Salminus* spp.[60].

328 Our modeling approaches on both chromosome evolution (ChromEvol) and
329 biogeographical patterns (BioGeoBEARS) support the ancestors of *Harttia* with a distribution
330 in either the Eastern Amazon or Southeast/South Atlantic drainages. The ancestral karyotype
331 was possibly composed of 2n = 58 chromosomes and an XY sex chromosome system, likely
332 in early stages of differentiation (Figure 5). Findings thus corroborate earlier hypotheses based
333 on comparative cytogenetics that proposed the same 2n as the ancestral state[21,61], therefore,
334 confirming the independent reductions of karyotypes from 2n = 58 to 2n = 56 in *H.*
335 *loricariformis*, *H. villasboas*, and *H. duriventris*, and subsequent reductions of 2n = 54 in *H.*
336 *rondoni* and *Harttia* sp. 3[23,24]. These karyotype reductions were mostly facilitated by centric
337 fusions, as indicated by our ChromEvol inference (Figure 4b, Supplementary Data 3).

Nevertheless, these chromosome rearrangements did not involve chromosomal components associated with the intricate multiple sex chromosome systems outlined in the genus[22,24]. The dissociation of autosomal and sex chromosomes dynamics underscores the intricate interaction of lineage-specific and conserved processes, such as Robertsonian translocations and inversions that influence chromosome evolution in this group. Notably, breakpoints in *Harttia* are probably linked to the instability of rDNA loci[20–24,28], particularly the 18S rDNA, which is not involved in the creation of the XY_1Y_2. Ribosomal sequences are known to compose evolutionary breakpoint regions among loricariids[62,63], since they increase genomic instability given the facilitated formation of double-strand breaks by the high transcriptional activity[64,65].

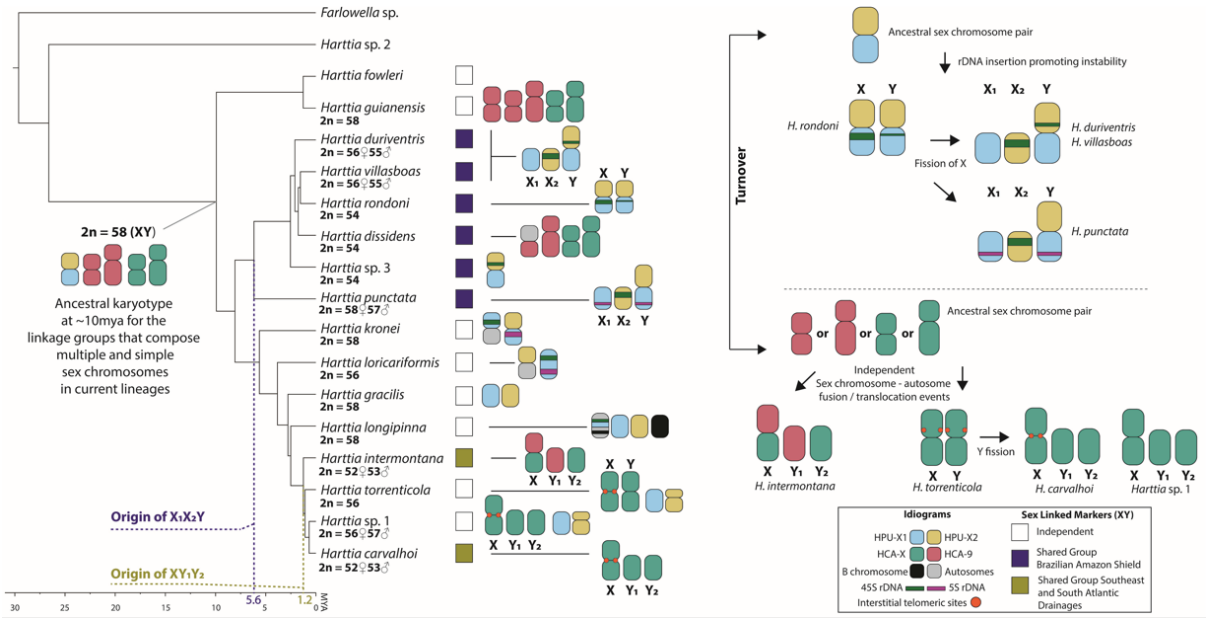

Figure 5. Rapid turnover of multiple sex chromosomes in *Harttia*. A compilation of previous cytogenetic data[18–28,61] and the results herein obtained with the main hypothesis for the sex chromosome evolution in *Harttia*. Chromosome colors follow the homology patterns established by Deon et al.[22,23] and Sassi et al.[24,28]. Idiograms are presented for each species-specific chromosome, while those pairs not shown in each species tip indicate the conservation of the ancestral state, as depicted on the left. Chromosomes are not drawn to scale.

Our study steer that recurrent turnover and independent evolution of multiple sex chromosomes are probably key mechanisms in the evolution of *Harttia*, reflecting the dynamic nature of sex chromosomes in this group. Across diverse lineages, including plants, fish, and reptiles, recurrent turnover of sex chromosomes within a relatively short evolutionary timescale has been reported[66–72], however, none is comparable with *Harttia*, where these events occur within a very short timeframe (~4 My). The arising of multiple sex chromosome systems usually results in postzygotic isolation, mainly due to segregation incompatibilities[7,11,73].

363 Rearrangements are also responsible for recombination suppression, which reduces gene flow
364 near rearranged regions[74–76]. Furthermore, genes that contribute to reproductive isolation can
365 accumulate on the neo-sex chromosomes, contributing to the speciation process[8,77]. We
366 hypothesize that a similar process may have happened on both rearrangement events, which
367 resulted in XY_1Y_2 and X_1X_2Y systems, leading to faster reproductive isolation and speciation.
368 This process was similarly documented in sticklebacks[8,77] and was also proposed for other
369 species such as *Brenthis* butterflies[78], African cichlids[79], and rock wallabies[80].
370 Among vertebrates, several mechanisms can drive sex chromosome turnover,
371 including the acquisition of novel sex-determining mutations, translocations of pre-existing sex-
372 determining (SD) genes, chromosomal fusions, and, in some cases, hybridization between
373 populations with distinct SD systems[8,11,67,81–86]. Given the absence of sympatric populations of
374 *Harttia*, turnover driven by hybridization events appears unlikely. Instead, the emergence of
375 the XY_1Y_2 system may be best explained by Y-autosome translocation, a mechanism widely
376 reported in teleosts with multiple sex chromosome systems[11]. In contrast, the X_1X_2Y systems
377 observed in clade II are more consistent with turnovers mediated either by novel SD mutations
378 or translocations of ancestral SD genes. Notably, the association of ribosomal DNA (rDNA)
379 sites with sex chromosomes in species of clade II suggests that rDNA insertions could act as
380 catalysts for recombination suppression by breaking the linkage groups of SD.
381 To validate the presence of sex linked markers, we cross-mapped the herein obtained
382 SLMs to the chromosome-level genome of *Pterygoplichtys pardalis* (divergence from *Harttia*
383 ~36 mya, according to TimeTree5[87]) revealing the large clusterization of those in chromosome
384 pairs 2 and 3 (Figure 3). Interestingly, pair 3 of *P. pardalis* results from a fusion of the catfish
385 ancestral microchromosomes 28 and 29 with the ancestral pair 6, carrying genes related to
386 basic cellular metabolism and genomic stability, to signal transduction and transcriptional
387 regulation[43]. Unfortunately, the study by Lv et al.[43] do not conduct any approach to investigate
388 putative sex chromosomes in *P. pardalis*, but the clusterization of *Harttia* SLM in two
389 chromosomes suggests that they may represent the two ancestral linkage groups responsible
390 for the origin of the two independently evolved sex chromosomes of *Harttia* (X_1X_2Y and XY_1Y_2).
391 Notably, our PCA analysis of SLM (Supplementary Figure 2) do not follow a clear pattern of
392 clusterization related to sex chromosome systems, indicating a big cluster formed by most
393 species and two independent clusters: one formed by *H. carvalhoi*, *H. torrenticola* and *Harttia*
394 sp. 1, and another by *H. intermontana*. This distribution indicates that most *Harttia* species
395 share similarities regarding SLMs and that the XY_1Y_2 has an independent evolutionary pattern,
396 also reinforced by the non-sharing SLMs (Figure 3).
397 In conclusion, our study presents the first genome-wide phylogenetic framework for the
398 armored catfish genus *Harttia*, offering new insights into its evolutionary history, chromosomal
399 evolution, and sex chromosome dynamics in teleosts. While broadly congruent with previous

400 hypotheses, our phylogeny reveals several key topological differences, likely attributable to the
401 increased resolution afforded by genome-wide data. Divergence time estimates highlight a
402 relatively recent radiation of *Harttia* sensu stricto over the past 10 million years, tightly
403 associated with major geological and hydrological transformations in South America driven by
404 the formation of the Amazon River and the rise of the mountain ranges, and potentially
405 accelerated by the rapid turnover of multiple sex chromosomes at 2.6 and 1.3 mya. Our results
406 further support the hypothesis that *Harttia* sp. 2, like *H. absaberi*, falls outside *Harttia* sensu
407 stricto, reflecting deep phylogenetic divergence corroborated by both cytogenetic and
408 molecular evidence, and challenging the monophyly of the genus. Chromosome evolution in
409 *Harttia* is characterized by a dynamic interplay of variation in diploid numbers, lineage-specific
410 reductions via centric fusions, and recurrent turnovers of sex chromosomes, leading to the
411 independent origins of complex multiple sex chromosome systems, which seem crucial in
412 establishing the diversity of the genus. Notably, the integration of sex-linked marker analysis
413 suggests that the evolution of sex chromosomes in *Harttia* is followed not only by structural
414 rearrangements but also by the recruitment of genes associated with reproductive and
415 physiological functions. Together, these findings underscore the potential contribution of
416 multiple sex chromosome systems and their turnovers in accelerating speciation rates when
417 compared to the simple chromosome system representatives. It also reveals the intricate
418 evolutionary processes shaping both genome structure and diversification in Neotropical
419 fishes. Future studies incorporating broader taxonomic and genomic sampling will be essential
420 to further refine the evolutionary history of *Harttia*, a remarkable repository of multiple sex
421 chromosome systems.
422

423 **4. Methods**

424 ***4.1 Sampling***

425 We selected all *Harttia* species with available cytogenetic data, following those
426 described in Supplementary Table 1. The sex of the individuals was recovered from the
427 morphological investigation of the gonads. Fish were anesthetized and euthanized with
428 Eugenol, as approved by the Ethics Committee on Animal Experimentation of the Universidade
429 Federal de São Carlos (Process number CEUA 7994170423). We have complied with all
430 relevant ethical regulations for animal use.
431

432 ***4.2 DArTseq and sex-linked markers***

433 Liver tissue samples were collected from six individuals of each species (three males
434 and three females), comprising a full dataset of 107 individuals, and submitted to Diversity
435 Arrays Technology (DArT) Pty Ltd (University of Canberra, Canberra, Australia) for genotyping
436 by sequencing. Briefly, DNA samples were digested with the restriction enzymes *PstI* and

437 *SphI*, followed by adapter ligation and 30 cycles of PCR amplification. Amplified products were
438 sequenced using single end reads on an Illumina HiSeq2000 platform. Data filtering and quality
439 control were performed by DArT Pty Ltd, excluding loci with reproducibility <90% and read
440 depths <3.5× for SNPs and <5× for Silico-DArT markers. For the characterization of sex-linked
441 markers, both SNPs and Silico-DArT loci with missing data were not included in the analysis.
442 For all remaining analyses (PCA, phylogenetic inference), loci with high frequencies of null
443 alleles (call rate <0.85) were filtered out.

444 Candidate sex-linked markers were identified following the pipeline proposed by
445 Lambert et al.[37]. DArTseq datasets were first organized per species and sex, grouping males
446 and females separately. For each individual, SNPs were tallied by heterozygous genotypes
447 (coded as "2") for each sex, using counts of homozygous genotypes (either "0" for the
448 reference or "1" for the alternate allele) as the baseline. Given that, sex-linked SNPs were
449 defined as SNPs with all individuals from one sex presenting heterozygous genotypes and all
450 individuals from the other sex with homozygous genotypes. On the other hand, sex linked
451 markers from Silico-DArT data (presence and absence) corresponded to those with the
452 presence of the restriction recognition sites in all individuals from one sex but not the other.

453 The theoretical per-species probability (P) of a SNP randomly assorting by sex purely
454 by chance is calculated as $P = 2^{(1-n)}$ [37], where n is the number of individuals of the minority sex
455 (here, n=3 for all species). This gives $P = 2^{(1-3)} = 0.25$. However, the DArTseq™ protocol
456 optimizes complexity-reduction chemistry at the sequencing plate level, meaning the same
457 genomic regions are interrogated for all samples on a plate. It selects a representative portion
458 of the dataset to verify which restriction enzymes better outcome a complexity reduction for
459 the whole species dataset. Considering that our SNP dataset comprised a total of 95,305 high-
460 confidence markers derived from the same plate chemistry, we used a method to create a
461 conservative genome-wide estimate of the false discovery rate by applying a Bonferroni
462 correction for multiple testing across this entire SNP dataset (N = 95,305). The corrected per-
463 test significance threshold was calculated as: $P_corrected = P/N = 0.25/95{,}305 \approx 2.62 \times 10^{-6}$.
464 This extremely stringent threshold means that any SNP exhibiting fixed sex-associated
465 differentiation in a species is highly unlikely to be a false positive. Seeking to validate the SLM
466 herein obtained, we also annotated the SLMs into the only chromosome-level available
467 genome of Loricariidae – *Pterygoplichthys pardalis* (ASM5023128v1) using the 'Annotate from
468 Reference' function from Geneious (Geneious Prime v2025.1, Dotmatics, Boston, USA) with
469 a minimum similarity threshold of 95%. The resulting annotation files for each chromosome
470 (Chr1-26.csv), which included genomic coordinates and feature types, were exported.
471 Subsequent data processing and visualization were conducted in R version 4.3.1, with a
472 custom ggplot2 visualization to plot the distribution of these markers and depicting

473 chromosomes as ideograms (grey horizontal bars) with individual sex-linked markers overlaid
474 as points.
475 To assess potential homology among sex-linked markers, multiple sequence
476 alignments were performed in Geneious (Geneious Prime v2025.1, Dotmatics, Boston, USA)
477 using the MUSCLE algorithm with default settings. Pairs of sequences exhibiting 100%
478 similarity were identified from the pairwise distance matrix using a custom R script.
479
480 ***4.3 Time-calibrated phylogeny and Principal Component Analysis***
481 We inferred the evolutionary history of *Harttia* species by Maximum Likelihood using
482 RAxML-ng[88]. After filtering out SNPs under selection (5 sequences) using Bayescan[89], a total
483 of 1,381 SNPs of 107 individuals from 18 species (17 *Harttia* + 1 *Farlowella*) were included in
484 the analysis, totalizing 24,858 markers. First, model selection was conducted in ModelTest-
485 NG[90] with seed number defined as "12345", and all models supported by RAxML-ng were
486 tested. ModelTest-NG indicated HKY+I+G4 as the model with the smallest AIC (lnL -
487 118802.5778) and HKY+I as the model with the lowest BIC (lnL 240039.7218). The analysis
488 was conducted with 50 initial maximum parsimony trees and 50 initial random trees. The
489 analysis was performed with a total of 1000 bootstraps and mapped into the best tree. The
490 tree with the highest log likelihood was used for time calibration. Finally, the tree was rooted
491 using FigTree v.1.4.4[91], defining *Farlowella* sp. as the outgroup.
492 Coalescent divergence times and population sizes were estimated under the
493 Multispecies Coalescent Model using BPP[92] and calibrated to geological time with bppR[93].
494 BPP is comprehensive software for Bayesian Markov Chain Monte Carlo (MCMC) analysis,
495 widely applied for species delimitation and divergence times estimation[92]. We first performed
496 an A00 method analysis (no species delimitation and fixed tree topology). To ensure the
497 consistency of the estimations in our dataset[94,95], we performed independent runs with random
498 subsets of different sizes (300, 400, and 500 SNPs), each with triplicates starting at distinct
499 seed numbers. We assumed a mutation rate (μ) of 3×10^{-9} based on the inferred rate of the
500 *Malapterurus electricus*, the closest Siluriformes with μ data[96]. We also adopted a divergence
501 time estimation of 30 mya for *Harttia* and *Farlowella* based on the mean of estimates on
502 TimeTree5[97]. Considering these values, the theta prior was defined as an inverse gamma
503 distribution of 3 0.002, and the tau prior was set as an inverse gamma distribution of 3 0.18.
504 For this analysis, *Farlowella* was defined as the outgroup. Finetune was allowed, chain length
505 was set to 400,000 generations, with a burn-in of 40,000, and sampling frequency was defined
506 as 2. The first 15% of the samples of each run were discarded as burn-in, and each triplicate
507 was concatenated. Effective sample size (ESS) values were checked on Tracer[91] to ensure
508 that posterior distributions were adequately estimated. The final time calibrations were defined
509 as the mean of the triplicate outputs with 95% HPD in bppR (Supplementary Table 2). We

510 performed a time calibration using a prior node age, based on the mean divergence time of
511 *Harttia* and *Farlowella* estimated on TimeTree5[97]. To describe the temporal patterns of
512 cladogenesis within the genus, we created a lineage-through-time plot (LTT plot) using ape
513 5.8[98] on R.
514 Principal component analysis (PCA) was conducted using the R package dartR[99,100].
515 Two distinct datasets were defined, one containing all sex-linked SNPs and a second using
516 the whole SNP dataset, excluding the sex-linked ones (here defined as autosomal SNPs). The
517 most representative PCs were selected for the plot, and the figure was constructed in Adobe
518 Illustrator (Adobe Corporation).
519
520 ***4.4 Character state-dependent branching***
521 We applied the Binary State Speciation and Extinction (BiSSE) model[101] in R (4.3.1)
522 with the package "hisse"[102] to test whether the presence of multiple sex chromosomes is
523 associated with differences in diversification rates. The binary dataset for the character
524 "multiple sex chromosomes" was defined with two states: absence = 0 and presence = 1. We
525 followed the strategy proposed in Lambert et al.[103], to estimate state-specific speciation rates
526 (λ_0 and λ_1), a single turnover rate ($\varepsilon = \mu/\lambda$) applied to both states, and a single transition rate
527 ($q_{0\leftrightarrow 1}$) between trait states. Likelihood optimization employed an initial simulated annealing
528 phase followed by refinement using a subplex routine to obtain maximum likelihood estimates
529 for speciation rates (λ_0, λ_1), a common turnover rate (ε), and transition rate ($q_{0\leftrightarrow 1}$). Confidence
530 intervals for parameter estimates were derived through likelihood profiling via the
531 SupportRegionHiSSE function, sampling 1000 points within the likelihood support region. To
532 assess whether differences in speciation rates between trait states were statistically significant,
533 we performed a likelihood ratio test (LRT). This involved comparing a full model where
534 speciation rates were allowed to vary between states ($\lambda_0 \neq \lambda_1$) to a constrained null model in
535 which speciation rates were set equal across states ($\lambda_0 = \lambda_1$). The test statistics were calculated
536 as twice the difference in log-likelihoods between the models, which was compared to a chi-
537 squared distribution with one degree of freedom, revealing a p-value of 0.005559656.
538
539 ***4.5 Chromosome number evolution***
540 Chromosome counts and a time-calibrated phylogenetic tree with branch lengths were
541 analyzed in ChromEvol v2.0[104] to infer ancestral chromosome numbers. We evaluated six
542 default models incorporating ascending dysploidy (single chromosome gains) and descending
543 dysploidy (single chromosome losses) under a time-homogeneous framework. Model
544 adequacy was assessed based on the best-fitting model (Dys). The minimum chromosome
545 number was set to n = 26, corresponding to the lowest value observed in both *Harttia carvalhoi*
546 and *H. intermontana*. The maximum chromosome number was set to n = 31, based on the

highest diploid count (2n = 62) recorded for *H. absaberi* and *Harttia* sp. 2, the latter included in our dataset.

4.6 Ancestral range estimation

The ancestral range of species was estimated using BioGeoBEARS[105], implemented in R. Three models of range evolution were tested: the dispersal–extinction–cladogenesis (DEC) model[106], the likelihood version of DIVA - DIVALIKE[107], and BAYAREALIKE[108]. Variants of these models incorporating a founder-event speciation parameter ("j") were not considered, as this parameter has been widely criticized[109] and is unlikely to accurately represent dispersal in freshwater-restricted taxa where river connectivity is essential for gene flow.

Six freshwater ecoregions were defined based on the present-day distribution of species included in the analysis: Western Amazon (W), Eastern Amazon (E), Amazon Brazilian Shield (B), São Francisco and Northeastern drainages (F), Southern and Southeastern Atlantic drainages (A), and the La Plata basin (L). Species distributions were compiled from original descriptions and related literature[110] and cross-referenced with occurrence data obtained from GBIF, which were visualized in QGIS (Supplementary Figure 4). Given the high endemism of *Harttia* species, which typically do not span multiple regions, we set the maximum number of areas allowed per node to two. This strategy avoids over-constraining the model, as using only a single area per node is not recommended[105].

To account for major historical changes in river connectivity, we defined three time slices based on Neotropical geological history, following frameworks established by Conde-Saldaña et al.[111]: >23 Mya, 23–10 Mya, and <10 Mya. These periods encompass key events in river capture and paleodrainage evolution of the Neotropical region[54,112–114]. The map representing these connections was created using QGIS 3.28.2-Firenze using merged ecoregions from Abell et al.[115].

4.7 Statistics and Reproducibility

All statistical analyses were performed as described in the Methods. We employed standard statistical practices, including multiple-testing correction (Bonferroni) for marker discovery, model selection (AIC/BIC) for phylogenetics, and likelihood-based hypothesis testing (BiSSE). Bayesian methods were checked for convergence (ESS > 200). Sample sizes for each experiment are provided in the relevant Methods subsections. All custom code used for data analysis, figure generation, and statistical testing is publicly available on GitHub (see Data Availability statement), ensuring the full reproducibility of this work.

Data and code availability

All the data and scripts used for this study are available at https://github.com/sassichico/harttia.

585 **References**

586 1. Muller, H. J. Genetic variability, twin hybrids and constant hybrids, in a case of balanced
587 lethal factors. *Genetics* **3**, 422 (1918). doi: 10.1186/s12864-024-10089-5.
588 2. Ohno, S. Differentiation of the Primitive Sex Elements at the Expense of the Y or W, and
589 the Conservation of the Original X or Z. in *Sex Chromosomes and Sex-linked Genes* (ed.
590 Ohno, S.) 13–24 (Springer, Berlin, Heidelberg, 1966). doi:10.1007/978-3-662-35113-0_6.
591 3. Graves, J. Sex Chromosome Specialization and Degeneration in Mammals. *Cell* **124**,
592 901–14 (2006). doi: 10.1016/j.cell.2006.02.024.
593 4. Zhu, Z., Younas, L. & Zhou, Q. Evolution and regulation of animal sex chromosomes. *Nat*
594 *Rev Genet* 1–16 (2024) doi:10.1038/s41576-024-00757-3.
595 5. Charlesworth, D., Barton, N. H. & Charlesworth, B. The sources of adaptive variation.
596 *Philos Trans R Soc Lond B Biol Sci* **284**, 20162864 (2017). doi: 10.1098/rstb.2016.0456.
597 6. Kratochvíl, L. *et al.* Expanding the classical paradigm: what we have learnt from
598 vertebrates about sex chromosome evolution. *Philos Trans R Soc Lond B Biol Sci* **376**,
599 20200097 (2021). doi: 10.1098/rstb.2020.0097.
600 7. White, M. The origin and evolution of multiple sex chromosome mechanisms. *Journal of*
601 *Genetics* 303–306 (1940).
602 8. Kitano, J. & Peichel, C. L. Turnover of sex chromosomes and speciation in fishes. *Environ*
603 *Biol Fishes* **94**, 549–558 (2012). doi: 10.1007/s10641-011-9853-8.
604 9. Pokorná, M., Altmanová, M. & Kratochvíl, L. Multiple sex chromosomes in the light of
605 female meiotic drive in amniote vertebrates. *Chromosome Res* **22**, 35–44 (2014). doi:
606 10.1007/s10577-014-9403-2.
607 10. Pennell, M. W. *et al.* Y Fuse? Sex Chromosome Fusions in Fishes and Reptiles. *PLoS*
608 *Genetics* **11**, 1–17 (2015). doi: 10.1371/journal.pgen.1005237.
609 11. Sember, A. *et al.* Multiple sex chromosomes in teleost fishes from a cytogenetic
610 perspective: state of the art and future challenges. *Philos Trans R Soc Lond B Biol Sci*
611 **376**, 20200098 (2021). doi: 10.1098/rstb.2020.0098.
612 12. Fricke, R., Eschmeyer, W. N. & van der Laan, R. *Eschmeyer's catalog of fishes: Genera,*
613 *Species, References*.
614 http://researcharchive.calacademy.org/research/ichthyology/catalog/fishcatmain.asp
615 (2025).
616 13. Covain, R. *et al.* Molecular phylogeny of the highly diversified catfish subfamily
617 Loricariinae (Siluriformes, Loricariidae) reveals incongruences with morphological
618 classification. *Mol Phylogenet Evol* **94**, 492–517 (2016). doi:
619 10.1016/j.ympev.2015.10.018.

14. Londoño-Burbano, A. & Reis, R. E. A combined molecular and morphological phylogeny of the Loricariinae (Siluriformes: Loricariidae), with emphasis on the Harttiini and Farlowellini. *PloS One* **16**, e0247747 (2021). doi: 10.1371/journal.pone.0247747.
15. Krysanov, E. & Demidova, T. Extensive karyotype variability of African fish genus *Nothobranchius* (Cyprinodontiformes). *Comp Cytogenet* **12**, 387 (2018). doi: 10.3897/CompCytogen.v12i3.25092.
16. Štundlová, J. *et al.* Sex chromosome differentiation via changes in the Y chromosome repeat landscape in African annual killifishes *Nothobranchius furzeri* and *N. kadleci*. *Chromosome Res* **30**, 309–333 (2022). doi: 10.1007/s10577-022-09707-3.
17. Hospodářská, M. *et al.* Multiple Origins of Sex Chromosomes in *Nothobranchius* Killifishes. *Mol Ecol* **34**, e70029 (2025). doi: 10.1111/mec.70029.
18. Centofante, L., Bertollo, L. A. C. & Moreira-Filho, O. Cytogenetic characterization and description of an XX/XY_1Y_2 sex chromosome system in catfish *Harttia carvalhoi* (Siluriformes, Loricariidae). *Cytogenet Genome Res* 320–324 (2006). doi: 10.1159/000089887.
19. Blanco, D. R. *et al.* Origin of the $X_1X_1X_2X_2/X_1X_2Y$ sex chromosome system of *Harttia punctata* (Siluriformes, Loricariidae) inferred from chromosome painting and FISH with ribosomal DNA markers. *Genetica* **142**, (2014). doi: 10.1007/s10709-014-9759-4.
20. Sassi, F. M. C. *et al.* Multiple sex chromosomes and evolutionary relationships in amazonian catfishes: The outstanding model of the genus *Harttia* (Siluriformes: Loricariidae). *Genes* **11**, (2020). doi: 10.3390/genes11101179.
21. Deon, G. A. *et al.* Highly Rearranged Karyotypes and Multiple Sex Chromosome Systems in Armored Catfishes from the Genus *Harttia* (Teleostei, Siluriformes). *Genes* **11**, (2020).
22. Deon, G. A. *et al.* Evolutionary breakpoint regions and chromosomal remodeling in *Harttia* (Siluriformes: Loricariidae) species diversification. *Genet Mol Biol* **45**, (2022). doi: 10.3390/genes11111366.
23. Deon, G. A. *et al.* Chromosomal Rearrangements and Origin of the Multiple XX/XY_1Y_2 Sex Chromosome System in *Harttia* Species (Siluriformes: Loricariidae). *Front Genet* **13**, (2022). doi: 10.3389/fgene.2022.877522.
24. Sassi, F. M. C. *et al.* Homeology of sex chromosomes in Amazonian *Harttia* armored catfishes supports the X-fission hypothesis for the X_1X_2Y sex chromosome system origin. *Sci Rep* **13**, 15756 (2023). doi: 10.1038/s41598-023-42617-w.
25. Deon, G. A. *et al.* The role of satellite DNAs in the chromosomal rearrangements and the evolution of the rare XY_1Y_2 sex system in *Harttia* (Siluriformes: Loricariidae). *J Hered* **115**, esae028 (2024) doi:10.1093/jhered/esae028. doi: 10.1093/jhered/esae028.

655 26. Sassi, F. M. C. *et al.* Independent evolution of satellite DNA sequences in homologous
656 sex chromosomes of Neotropical armored catfish (*Harttia*). *Commun Biol* **8**, 524 (2025).
657 doi: 10.1038/s42003-025-07891-6.
658 27. Sassi, F. M. C. *et al.* Adding New Pieces to the Puzzle of Karyotype Evolution in *Harttia*
659 (Siluriformes, Loricariidae): Investigation of Amazonian Species. *Biology* **10**, (2021). doi:
660 10.3390/biology10090922.
661 28. Sassi, F. M. C. *et al.* Turnover of multiple sex chromosomes in *Harttia* catfish
662 (Siluriformes, Loricariidae): a glimpse from whole chromosome painting. *Front. Genet.*
663 **14**, 1226222 (2023). doi: 10.3389/fgene.2023.1226222.
664 29. Nedoluzhko, A. *et al.* Genomic evidence supports the introgression between two
665 sympatric stickleback species inhabiting the White Sea basin. *Heliyon* **7**, (2021). doi:
666 10.1016/j.heliyon.2021.e06160.
667 30. Kirschner, P. *et al.* Congruent evolutionary responses of European steppe biota to late
668 Quaternary climate change. *Nat Commun* **13**, 1921 (2022). doi: 10.1038/s41467-022-
669 29267-8.
670 31. Suchan, T. *et al.* A trans-oceanic flight of over 4,200 km by painted lady butterflies. *Nat*
671 *Commun* **15**, 5205 (2024). doi: 10.1038/s41467-024-49079-2
672 32. Davey, J. W. *et al.* Genome-wide genetic marker discovery and genotyping using next-
673 generation sequencing. *Nat Rev Genet* **12**, 499–510 (2011). doi: 10.1038/nrg3012.
674 33. Mirarab, S., Bayzid, M. S. & Warnow, T. Evaluating Summary Methods for Multilocus
675 Species Tree Estimation in the Presence of Incomplete Lineage Sorting. *Syst Biol* **65**,
676 366–380 (2016). doi: 10.1093/sysbio/syu063
677 34. Simmons, M. P. & Gatesy, J. Collapsing dubiously resolved gene-tree branches in
678 phylogenomic coalescent analyses. *Mol Phylogenet Evol* **158**, 107092 (2021). doi:
679 10.1016/j.ympev.2021.107092.
680 35. Jaccoud, D., Peng, K., Feinstein, D. & Kilian, A. Diversity arrays: a solid state technology
681 for sequence information independent genotyping. *Nucleic Acids Res* **29**, e25–e25
682 (2001). doi: 10.1093/nar/29.4.e25.
683 36. Wenzl, P. *et al.* Diversity Arrays Technology (DArT) for whole-genome profiling of barley.
684 *Proc Natl Acad Sci USA* **101**, 9915–9920 (2004). doi: 10.1073/pnas.0401076101.
685 37. Lambert, M. R., Skelly, D. K. & Ezaz, T. Sex-linked markers in the North American green
686 frog (*Rana clamitans*) developed using DArTseq provide early insight into sex
687 chromosome evolution. *BMC Genomics* **17**, 844 (2016). doi: 10.1186/s12864-016-3209-
688 x.
689 38. Sopniewski, J., Shams, F., Scheele, B. C., Kefford, B. J. & Ezaz, T. Identifying sex-linked
690 markers in *Litoria aurea*: a novel approach to understanding sex chromosome evolution
691 in an amphibian. *Sci Rep* **9**, 16591 (2019). doi: 10.1038/s41598-019-52970-4.

39. Baloch, F. S. *et al.* A Whole Genome DArTseq and SNP Analysis for Genetic Diversity Assessment in Durum Wheat from Central Fertile Crescent. *PLoS One* **12**, e0167821 (2017). doi: 10.1371/journal.pone.0167821.
40. Melville, J. *et al.* Identifying hybridization and admixture using SNPs: application of the DArTseq platform in phylogeographic research on vertebrates. *R Soc Open Sci* **4**, 161061 (2017). doi: 10.1098/rsos.161061.
41. Aznar-Fernández, T. *et al.* Identification of quantitative trait loci (QTL) controlling resistance to pea weevil (*Bruchus pisorum*) in a high-density integrated DArTseq SNP-based genetic map of pea. *Sci Rep* **10**, 33 (2020). doi: 10.1038/s41598-019-56987-7.
42. Mujyambere, V., Adomako, K. & Olympio, O. S. Effectiveness of DArTseq markers application in genetic diversity and population structure of indigenous chickens in Eastern Province of Rwanda. *BMC Genomics* **25**, 193 (2024). doi: 10.1186/s12864-024-10089-5.
43. Lv, Y. *et al.* Chromosome-level genome assembly reveals adaptive evolution of the invasive Amazon sailfin catfish (*Pterygoplichthys pardalis*). *Commun Biol* **8**, 616 (2025). doi: 10.1038/s42003-025-08029-4.
44. Dagosta, F. C. P. & Pinna, M. de. Biogeography of Amazonian fishes: deconstructing river basins as biogeographic units. *Neotrop Ichthyol* **15**, (2017). doi: 10.1590/1982-0224-20170034.
45. Dagosta, F. C. P. & Pinna, M. D. The Fishes of the Amazon: Distribution and Biogeographical Patterns, with a Comprehensive List of Species. *Bull Am Mus Nat Hist* **2019**, 1–163 (2019). doi: 10.1206/0003-0090.431.1.1.
46. Dutra, G. *et al.* Rapid assessment of the ichthyofauna of the southern Guiana Shield tributaries of the Amazonas River in Pará, Brazil. *Acta Amazonica* **50**, 24–36 (2020). doi: 10.1590/1809-4392201901402.
47. Rapp Py-Daniel, L. H. & Oliveira, E. C. Seven new species of *Harttia* from the Amazonian-Guyana region (Siluriformes: Loricariidae). *Ichthyol Explor Freshw* **12**, 79–96 (2001).
48. Pomara, L. Y., Ruokolainen, K. & Young, K. R. Avian species composition across the Amazon River: the roles of dispersal limitation and environmental heterogeneity. *J Biogeogr* **41**, 784–796 (2014). doi: 10.1111/jbi.12247.
49. Godinho, M. B. de C. & da Silva, F. R. The influence of riverine barriers, climate, and topography on the biogeographic regionalization of Amazonian anurans. *Sci Rep* **8**, 3427 (2018). doi: 10.1038/s41598-018-21879-9.
50. Naka, L. N., Costa, B. M. da S., Lima, G. R. & Claramunt, S. Riverine Barriers as Obstacles to Dispersal in Amazonian Birds. *Front Ecol Evol* **10**, (2022). doi: 10.3389/fevo.2022.846975.
51. Rodrigues, R. M. *Estudos cromossômicos e moleculares em Loricariinae com ênfase em espécies de Rineloricaria (Siluriformes, Loricariidae): uma perspectiva evolutiva.*

729 *Universidade de São Paulo*. https://www.teses.usp.br/teses/disponiveis/41/41131/tde-
730 17122010-104716/publico/Raque_Maria_Rodrigues.pdf (2010).
731 52. Cherobim, A. M. *UNESP. Phylogenetic analysis of Harttia Steindachner, 1877*
732 *(Siluriformes: Loricariidae: Loricariinae)*. http://hdl.handle.net/11449/216922 (2021).
733 53. Hubert, N. & Renno, J.-F. Historical biogeography of South American freshwater fishes.
734 *J Biogeogr* **33**, 1414–1436 (2006). doi: 10.1111/j.1365-2699.2006.01518.x.
735 54. Albert, J. S., Val, P. & Hoorn, C. The changing course of the Amazon River in the
736 Neogene: center stage for Neotropical diversification. *Neotrop Ichthyol* **16**, (2018). doi:
737 10.1590/1982-0224-20180033.
738 55. Roxo, F. F. *et al.* Phylogenomic reappraisal of the Neotropical catfish family Loricariidae
739 (Teleostei: Siluriformes) using ultraconserved elements. *Mol Phylogenet Evol* **135**, 148–
740 165 (2019). doi: 10.1016/j.ympev.2019.02.017.
741 56. Dagosta, F. C. P., de Pinna, M., Peres, C. A. & Tagliacollo, V. A. Existing protected areas
742 provide a poor safety-net for threatened Amazonian fish species. *Aquat Conserv* **31**,
743 1167–1189 (2021). doi: 10.1002/aqc.3461.
744 57. Costa, W. J. E. M. Historical biogeography of cynolebiasine annual killifishes inferred from
745 dispersal–vicariance analysis. *J Biogeogr* **37**, 1995–2004 (2010). doi: 10.1111/j.1365-
746 2699.2010.02339.x.
747 58. Cassemiro, F. A. S. *et al.* Landscape dynamics and diversification of the megadiverse
748 South American freshwater fish fauna. *Proc Natl Acad Sci USA* **120**, e2211974120
749 (2023). doi: 10.1073/pnas.2211974120.
750 59. Cassemiro, F. A. S., Salgado, A. A. R., Paixão, R. W. & Rezende, É. A. The timing of
751 large drainage rearrangement in South America: A study based on morphological and
752 ecological evidence. *Geomorphology* **468**, 109457 (2025). doi:
753 10.1016/j.geomorph.2024.109457.
754 60. Machado, C. B., Galetti Jr, P. M. & Carnaval, A. C. Bayesian analyses detect a history of
755 both vicariance and geodispersal in Neotropical freshwater fishes. *J Biogeogr* **45**, 1313–
756 1325 (2018). doi: 10.1111/jbi.13207.
757 61. Blanco, D. R. *et al.* Karyotype Diversity and Evolutionary Trends in Armored Catfish
758 Species of the Genus *Harttia* (Siluriformes: Loricariidae). *Zebrafish* **14**, 169–176 (2017).
759 62. Barros, A. V. *et al.* Fragile sites, dysfunctional telomere and chromosome fusions: What
760 is 5S rDNA role? *Gene* **608**, 20–27 (2017). doi: 10.1016/j.gene.2017.01.013.
761 63. Glugoski, L., Giuliano-Caetano, L., Moreira-Filho, O., Vicari, M. R. & Nogaroto, V. Co-
762 located hAT transposable element and 5S rDNA in an interstitial telomeric sequence
763 suggest the formation of Robertsonian fusion in armored catfish. *Gene* **650**, 49–54
764 (2018). doi: 10.1016/j.gene.2018.01.099.

765 64. Berthelot, C., Muffato, M., Abecassis, J. & Crollius, H. R. The 3D organization of
766 chromatin explains evolutionary fragile genomic regions. *Cell Rep* **10**, 1913–1924 (2015).
767 doi: 10.1016/j.celrep.2015.02.046.
768 65. Warmerdam, D. O. & Wolthuis, R. M. F. Keeping ribosomal DNA intact: a repeating
769 challenge. *Chrom Res* **27**, 57–72 (2019). doi: 10.1007/s10577-018-9594-z.
770 66. Keating, S. E. *et al.* Sex Chromosome Turnover in Bent-Toed Geckos (*Cyrtodactylus*).
771 *Genes* **12**, 116 (2021). doi: 10.3390/genes12010116.
772 67. Kabir, A. *et al.* Repeated translocation of a supergene underlying rapid sex chromosome
773 turnover in *Takifugu* pufferfish. *Proc Natl Acad Sci USA* **119**, e2121469119 (2022). doi:
774 10.1073/pnas.2121469119.
775 68. Huang, Z. *et al.* Recurrent chromosome reshuffling and the evolution of neo-sex
776 chromosomes in parrots. *Nature Communications* **13**, 944 (2022). doi: 10.1038/s41467-
777 022-28585-1.
778 69. Yi, X. *et al.* Sex chromosome turnover in hybridizing stickleback lineages. *Evol Lett* **8**,
779 658–668 (2024). doi: 10.1093/evlett/qrae019.
780 70. Hayashi, S. *et al.* Sex chromosome cycle as a mechanism of stable sex determination. *J*
781 *Biochem* **176**, 81–95 (2024). doi: 10.1093/jb/mvae045.
782 71. Wang, J., Tao, W., Kocher, T. D. & Wang, D. Sex chromosome turnover and biodiversity
783 in fishes. *J Genet Genomics* **51**, 1351–1360 (2024). doi: 10.1016/j.jgg.2024.08.008
784 72. Zheng, S. *et al.* The origin, evolution, and translocation of sex chromosomes in *Silurus*
785 catfish mediated by transposons. *BMC Biol* **23**, 54 (2025). doi: 10.1186/s12915-025-
786 02160-8.
787 73. Furman, B. L. S. *et al.* Sex Chromosome Evolution: So Many Exceptions to the Rules.
788 *Genome Biol Evol* **12**, 750–763 (2020). doi: 10.1093/gbe/evaa081.
789 74. Yannic, G., Basset, P. & Hausser, J. Chromosomal rearrangements and gene flow over
790 time in an inter-specific hybrid zone of the *Sorex araneus* group. *Heredity* **102**, 616–625
791 (2009). doi: 10.1038/hdy.2009.19.
792 75. McGaugh, S. E. & Noor, M. A. F. Genomic impacts of chromosomal inversions in
793 parapatric *Drosophila* species. *Philos Trans R Soc Lond B Biol Sci* **367**, 422–429 (2012).
794 doi: 10.1098/rstb.2011.0250.
795 76. Toups, M. A., Rodrigues, N., Perrin, N. & Kirkpatrick, M. A reciprocal translocation
796 radically reshapes sex-linked inheritance in the common frog. *Mol Ecol* **28**, 1877–1889
797 (2019). doi: 10.1111/mec.14990
798 77. Kitano, J. *et al.* A role for a neo-sex chromosome in stickleback speciation. *Nature* **461**,
799 1079–1083 (2009). doi: 10.1038/nature08441.

800 78. Mackintosh, A., Vila, R., Martin, S. H., Setter, D. & Lohse, K. Chromosome fissions and
801 fusions act as barriers to gene flow between *Brenthis* fritillary butterflies. *Mol Biol Evol* **40**,
802 msad043 (2023) doi: 10.1093/molbev/msad043.
803 79. El Taher, A., Ronco, F., Matschiner, M., Salzburger, W. & Böhne, A. Dynamics of sex
804 chromosome evolution in a rapid radiation of cichlid fishes. *Sci Adv* **7**, eabe8215. doi:
805 10.1126/sciadv.abe8215.
806 80. Potter, S. *et al.* Chromosomal Speciation in the Genomics Era: Disentangling
807 Phylogenetic Evolution of Rock-wallabies. *Front Genet* **8**, (2017). doi:
808 10.3389/fgene.2017.00010.
809 81. Yoshida, K. & Kitano, J. Tempo and mode in karyotype evolution revealed by a
810 probabilistic model incorporating both chromosome number and morphology. *PLoS*
811 *Genet* **17**, e1009502 (2021). doi: 10.1111/j.1558-5646.2012.01681.x.
812 82. Graves, J. A. M. Evolution of vertebrate sex chromosomes and dosage compensation.
813 *Nat Rev Genet* **17**, 33–46 (2016). doi: 10.1038/nrg.2015.2.
814 83. Palmer, D. H., Rogers, T. F., Dean, R. & Wright, A. E. How to identify sex chromosomes
815 and their turnover. *Mol Ecol* **28**, 4709–4724 (2019). doi: 10.1111/mec.15245.
816 84. Bracewell, R. & Bachtrog, D. Complex Evolutionary History of the Y Chromosome in Flies
817 of the *Drosophila obscura* Species Group. *Genome Biol Evol* **12**, 494–505 (2020). doi:
818 10.1093/gbe/evaa051.
819 85. Bracewell, R., Chatla, K., Nalley, M. J. & Bachtrog, D. Dynamic turnover of centromeres
820 drives karyotype evolution in *Drosophila*. *Elife* **8**, e49002 (2019). doi:
821 10.7554/eLife.49002.
822 86. Faber-Hammond, J. J., Phillips, R. B. & Brown, K. H. Comparative Analysis of the Shared
823 Sex-Determination Region (SDR) among Salmonid Fishes. *Genome Biol Evol* **7**, 1972–
824 1987 (2015). doi: 10.1093/gbe/evv123.
825 87. Kumar, S., Stecher, G., Suleski, M. & Hedges, S. B. TimeTree: A Resource for Timelines,
826 Timetrees, and Divergence Times. *Mol Biol Evol* **34**, 1812–1819 (2017). doi:
827 10.1093/molbev/msac174.
828 88. Stamatakis, A. RAxML version 8: a tool for phylogenetic analysis and post-analysis of
829 large phylogenies. *Bioinformatics* **30**, 1312–1313 (2014). doi:
830 10.1093/bioinformatics/btu033.
831 89. Foll, M. & Gaggiotti, O. A Genome-Scan Method to Identify Selected Loci Appropriate for
832 Both Dominant and Codominant Markers: A Bayesian Perspective. *Genetics* **180**, 977–
833 993 (2008). doi: 10.1534/genetics.108.092221.
834 90. Darriba, D. *et al.* ModelTest-NG: A New and Scalable Tool for the Selection of DNA and
835 Protein Evolutionary Models. *Mol Biol Evol* **37**, 291–294 (2020). doi:
836 10.1093/molbev/msz189.

837 91. Rambaut, A., Drummond, A. J., Xie, D., Baele, G. & Suchard, M. A. Posterior
838 Summarization in Bayesian Phylogenetics Using Tracer 1.7. *Syst Biol* **67**, 901–904
839 (2018). doi: 10.1093/sysbio/syy032.
840 92. Yang, Z. The BPP program for species tree estimation and species delimitation. *Curr Zool*
841 **61**, 854–865 (2015). doi: 10.1093/czoolo/61.5.854.
842 93. Angelis, K. & Dos Reis, M. The impact of ancestral population size and incomplete
843 lineage sorting on Bayesian estimation of species divergence times. *Curr Zool* **61**, 874–
844 885 (2015). doi: 10.1093/czoolo/61.5.874.
845 94. Flouri, T., Jiao, X., Rannala, B. & Yang, Z. Species Tree Inference with BPP Using
846 Genomic Sequences and the Multispecies Coalescent. *Mol Biol Evol* **35**, 2585–2593
847 (2018). doi: 10.1093/molbev/msy147
848 95. Tiley, G. P., Poelstra, J. W., Dos Reis, M., Yang, Z. & Yoder, A. D. Molecular Clocks
849 without Rocks: New Solutions for Old Problems. *Trends Genet* **36**, 845–856 (2020). doi:
850 10.1016/j.tig.2020.06.002.
851 96. Liu, M. *et al.* A chromosome-level genome of electric catfish (*Malapterurus electricus*)
852 provided new insights into order Siluriformes evolution. *Mar Life Sci Technol* **6**, 1–14
853 (2024). doi: 10.1007/s42995-023-00197-8.
854 97. Kumar, S. *et al.* TimeTree 5: An Expanded Resource for Species Divergence Times. *Mol*
855 *Biol Evol* **39**, msac174 (2022). doi: 10.1093/molbev/msac174.
856 98. Paradis, E. & Schliep, K. ape 5.0: an environment for modern phylogenetics and
857 evolutionary analyses in R. *Bioinformatics* **35**, 526–528 (2019). doi:
858 10.1093/bioinformatics/bty633.
859 99. Gruber, B., Unmack, P. J., Berry, O. F. & Georges, A. dartr: An r package to facilitate
860 analysis of SNP data generated from reduced representation genome sequencing. *Mol*
861 *Ecol Res* **18**, 691–699 (2018). doi: 10.1111/1755-0998.12745.
862 100. Mijangos, J.L., Gruber, B., Berry, O., Pacioni C., & Georges, A. dartR v2: An accessible
863 genetic analysis platform for conservation, ecology and agriculture. *Methods Ecol Evol*
864 **13**, 2150-2158 (2022). doi: 10.1111/2041-210X.13918. doi: 10.1111/2041-210X.13918.
865 101. Maddison, W. P., Midford, P. E. & Otto, S. P. Estimating a Binary Character's Effect on
866 Speciation and Extinction. *Syst Biol* **56**, 701–710 (2007). doi:
867 10.1080/10635150701607033.
868 102. Beaulieu, J. M. & O'Meara, B. C. Detecting Hidden Diversification Shifts in Models of
869 Trait-Dependent Speciation and Extinction. *Syst Biol* **65**, 583–601 (2016). doi:
870 10.1093/sysbio/syw022.
871 103. Lambert, S., Voznica, J. & Morlon, H. Deep Learning from Phylogenies for Diversification
872 Analyses. *Syst Biol* **72**, 1262–1279 (2023). doi: 10.1093/sysbio/syad044.

104. Glick, L. & Mayrose, I. ChromEvol: Assessing the Pattern of Chromosome Number Evolution and the Inference of Polyploidy along a Phylogeny. *Mol Biol Evol* **31**, 1914–1922 (2014). doi: 10.1093/molbev/msu122.
105. Matzke, N. J. BioGeoBEARS: BioGeography with Bayesian (and likelihood) Evolutionary Analysis with R Scripts. version 1.1.1. *GitHub* http://dx.doi.org/10.5281/zenodo.1478250 (2018).
106. Ree, R. H. & Smith, S. A. Maximum Likelihood Inference of Geographic Range Evolution by Dispersal, Local Extinction, and Cladogenesis. *Sys Biol* **57**, 4–14 (2008). doi: 10.1080/10635150701883881.
107. Ronquist, F. Dispersal-Vicariance Analysis: A New Approach to the Quantification of Historical Biogeography. *Syst Biol* **46**, 195–203 (1997). doi: 10.1093/sysbio/46.1.195.
108. Landis, M. J., Matzke, N. J., Moore, B. R. & Huelsenbeck, J. P. Bayesian Analysis of Biogeography when the Number of Areas is Large. *Syst Biol* **62**, 789–804 (2013). doi: 10.1023/A:1013379521338.
109. Ree, R. H. & Sanmartín, I. Conceptual and statistical problems with the DEC+J model of founder-event speciation and its comparison with DEC via model selection. *J Biogeogr* **45**, 741–749 (2018). doi: 10.1111/jbi.13173.
110. Oyakawa, O. T., Fichberg, I. & Py-Daniel, L. R. Three new species of *Harttia* (Loricariidae: Loricariinae) from Serra do Cachimbo, Rio Xingu basin, Pará, Northern Brazil. *Zootaxa* **4387**, 75–90 (2018). doi: 10.11646/zootaxa.4387.1.3.
111. Conde-Saldaña, C. C. *et al.* Landscape Evolution Drives Continental Diversification in Neotropical Freshwater Fishes of the Family Erythrinidae (Teleostei, Characiformes). *J Biogeogr* **52**, e15129 (2025). doi: 10.1111/jbi.15129.
112. Tagliacollo, V. A., Roxo, F. F., Duke-Sylvester, S. M., Oliveira, C. & Albert, J. S. Biogeographical signature of river capture events in Amazonian lowlands. *J Biogeogr* **42**, 2349–2362 (2015). doi: 10.1111/jbi.12594.
113. Montes, C. *et al.* A Middle to Late Miocene Trans-Andean Portal: Geologic Record in the Tatacoa Desert. *Front Earth Sci* **8**, (2021). doi: 10.3389/feart.2020.587022.
114. Albert, J. S. *et al.* Late Neogene megariver captures and the Great Amazonian Biotic Interchange. *Glob Planet Change* **205**, 103554 (2021). doi: 10.1016/j.gloplacha.2021.103554.
115. Abell, R. *et al.* Freshwater Ecoregions of the World: A New Map of Biogeographic Units for Freshwater Biodiversity Conservation. *Bioscience* **58**, 403-414 (2008). doi: 10.1641/B580507.

Acknowledgements

We appreciate the contributions of Osvaldo Oyakawa, Lúcia Rapp-Py Daniel for the identification of species used in this work, and to Claudio Oliveira, Vladimir Trifonov, José Maurício Barbanti Duarte, Francisco Langeani, and Orlando Moreira Filho for the valuable insights. We also thank Eliana Feldberg and all members of Laboratório de Genética Animal - INPA, so as Marcelo Vicari, Luiz Henrique Silva, and Antonio Donizete, for the assistance in collecting specimens. FMCS is funded by Conselho Nacional de Desenvolvimento Científico e Tecnológico (PDE-CNPq 200247/2025-5) and was supported during part this study by FAPESP 2020/02681-9, 2022/04261-2, and 2023/08116-0. MBC was supported by FAPESP (2023/00955-2). We also acknowledge the support by German Research Foundation Projekt-No. 512648189 (T.L.) and the Open Access Publication Fund of the Thueringer Universitaets- und Landesbibliothek Jena.

Author contributions

FMCS, FHSS, and MBC conceived and designed research. FMCS, FHSS, FS, and GAD conducted experiments. FMCS, FHSS, MFP, FS, and LX analyzed the data. MFP, TE, TL, LX, and MBC contributed with new methods. FMCS, FHSS, MFP, FS, TE, TL, GAD, LX, and MBC wrote the paper.

Competing interests

The authors declare no competing interests.

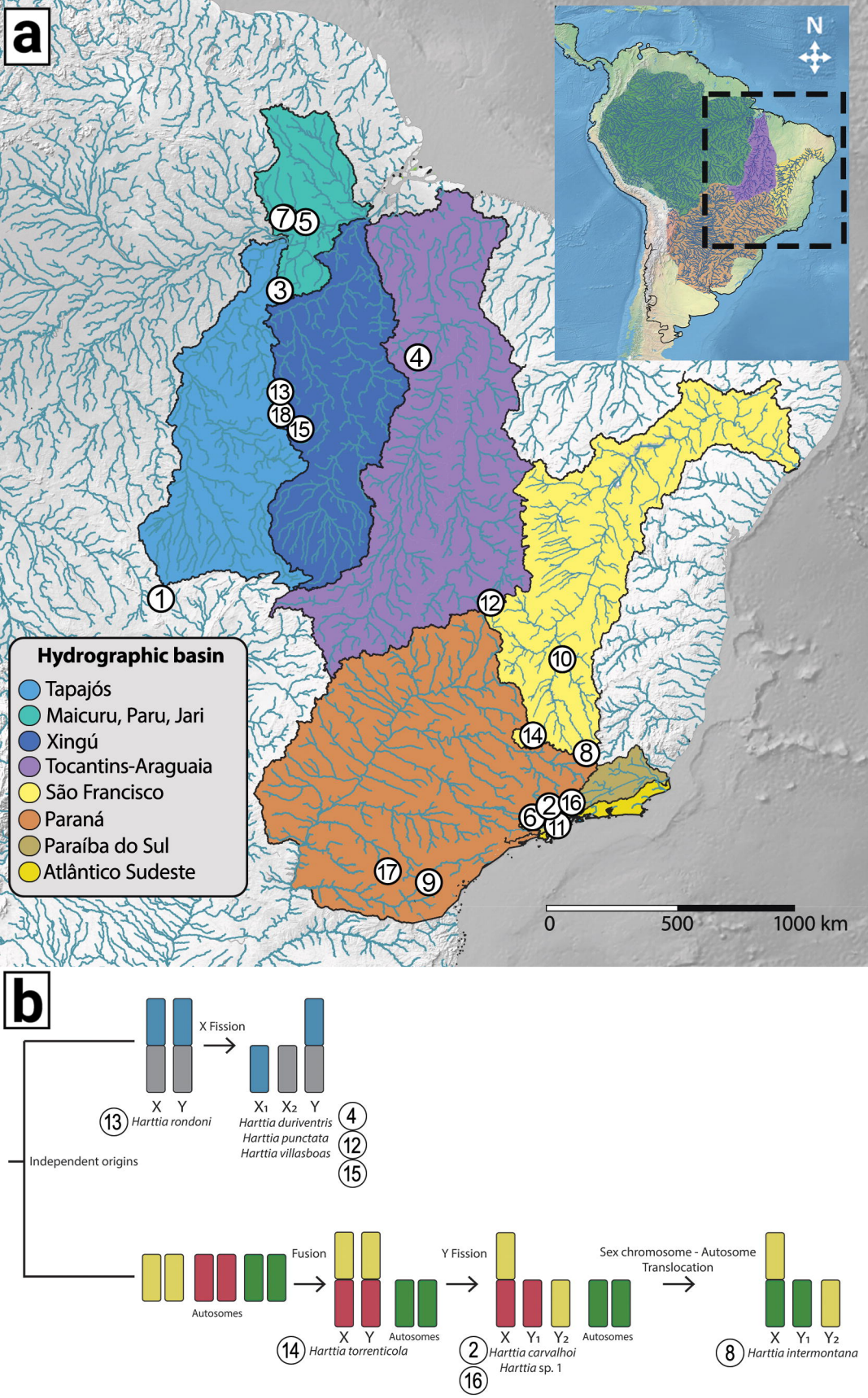
a
N
Hydrographic basin
Tapajós
Maicuru, Paru, Jari
Xingú
Tocantins-Araguaia
São Francisco
Paraná
Paraíba do Sul
Atlântico Sudeste
0
500
1000 km
b
X Fission
X Y
13 Harttia rondoni
X1 X2 Y
Harttia duriventris
Harttia punctata
Harttia villasboas
4
12
15
Independent origins
Autosomes
Fusion
X Y Autosomes
14 Harttia torrenticola
Y Fission
X Y1 Y2 Autosomes
2 Harttia carvalhoi
Harttia sp. 1
16
Sex chromosome - Autosome
Translocation
X Y1 Y2
8 Harttia intermontana

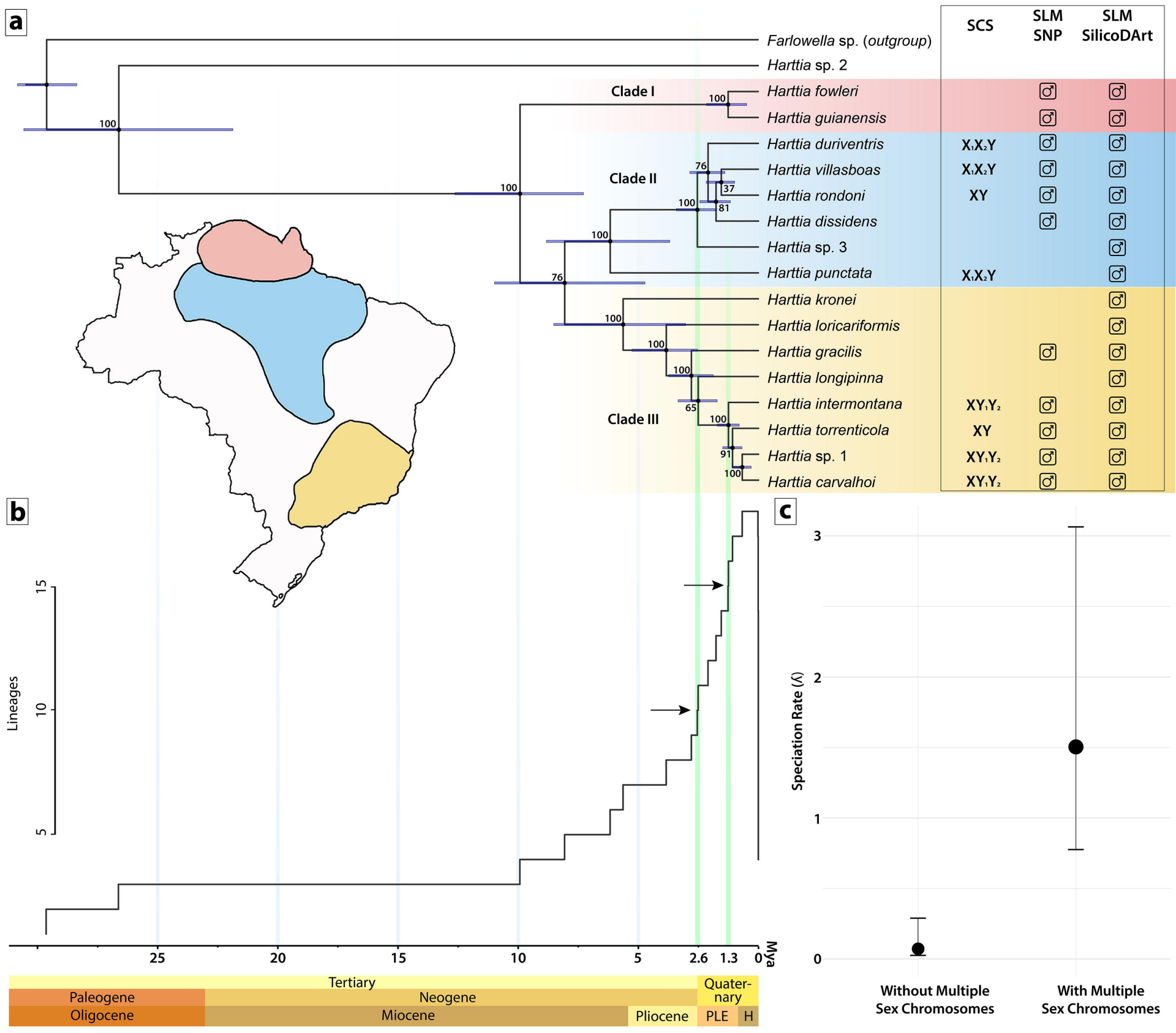
a
SCS
SLM SNP
SLM SilicoDArt
Farlowella sp. (outgroup)
Harttia sp. 2
Clade I
Harttia fowleri
Harttia guianensis
Clade II
Harttia duriventris
Harttia villasboas
Harttia rondoni
Harttia dissidens
Harttia sp. 3
Harttia punctata
Clade III
Harttia kronei
Harttia loricariformis
Harttia gracilis
Harttia longipinna
Harttia intermontana
Harttia torrenticola
Harttia sp. 1
Harttia carvalhoi
X1X2Y
X1X2Y
XY
X1X2Y
XY1Y2
XY
XY1Y2
XY1Y2
100
76
37
81
65
91
b
Lineages
Mya
Tertiary
Quaternary
Paleogene
Neogene
Oligocene
Miocene
Pliocene
PLE
H
c
Speciation Rate (λ)
Without Multiple Sex Chromosomes
With Multiple Sex Chromosomes

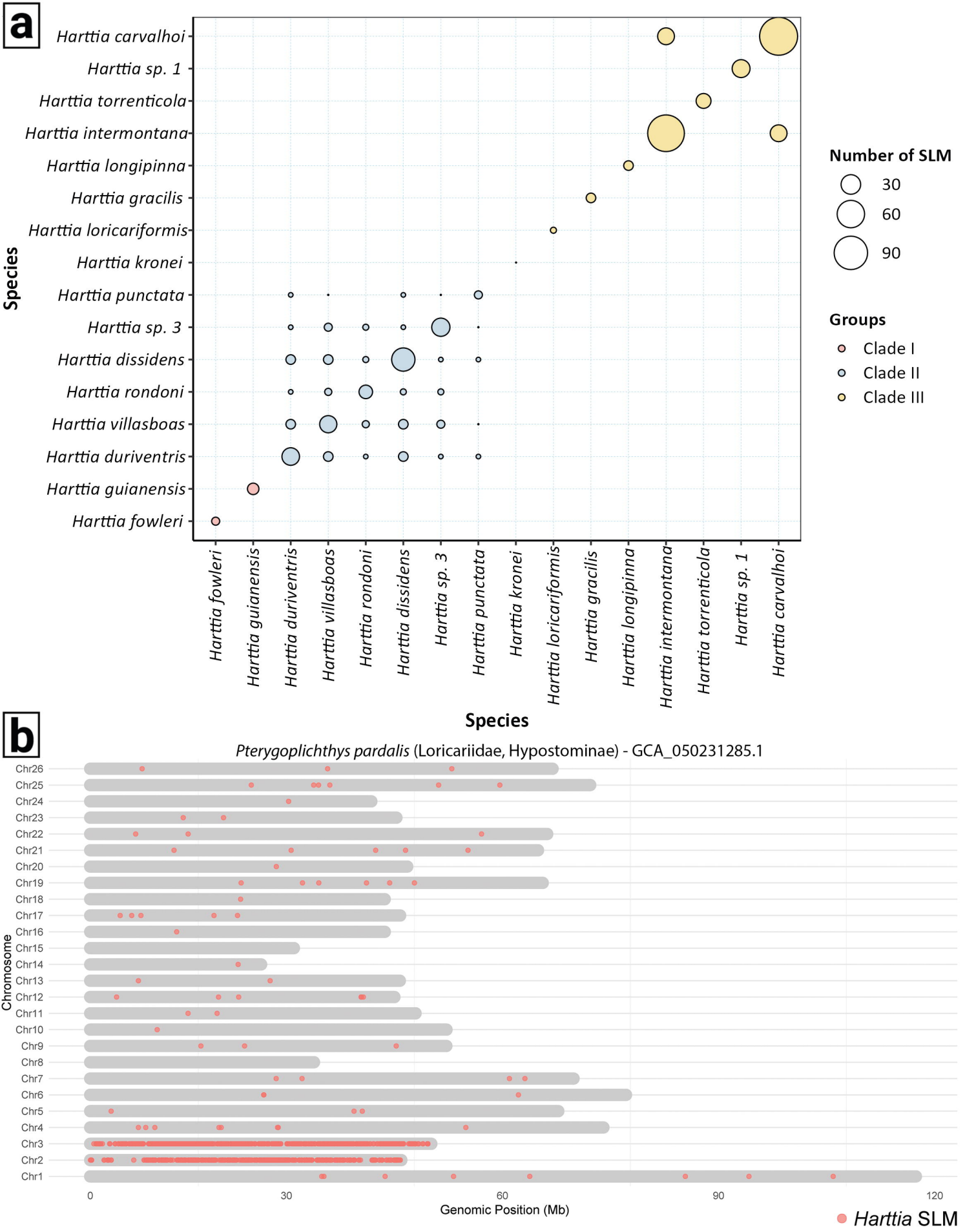
a
Harttia carvalhoi
Harttia sp. 1
Harttia torrenticola
Harttia intermontana
Harttia longipinna
Harttia gracilis
Harttia loricariformis
Harttia kronei
Harttia punctata
Harttia sp. 3
Harttia dissidens
Harttia rondoni
Harttia villasboas
Harttia duriventris
Harttia guianensis
Harttia fowleri
Species
Number of SLM
30
60
90
Groups
Clade I
Clade II
Clade III
b
Pterygoplichthys pardalis (Loricariidae, Hypostominae) - GCA_050231285.1
Chromosome
Chr26
Chr25
Chr24
Chr23
Chr22
Chr21
Chr20
Chr19
Chr18
Chr17
Chr16
Chr15
Chr14
Chr13
Chr12
Chr11
Chr10
Chr9
Chr8
Chr7
Chr6
Chr5
Chr4
Chr3
Chr2
Chr1
0
30
60
90
120
Genomic Position (Mb)
Harttia SLM

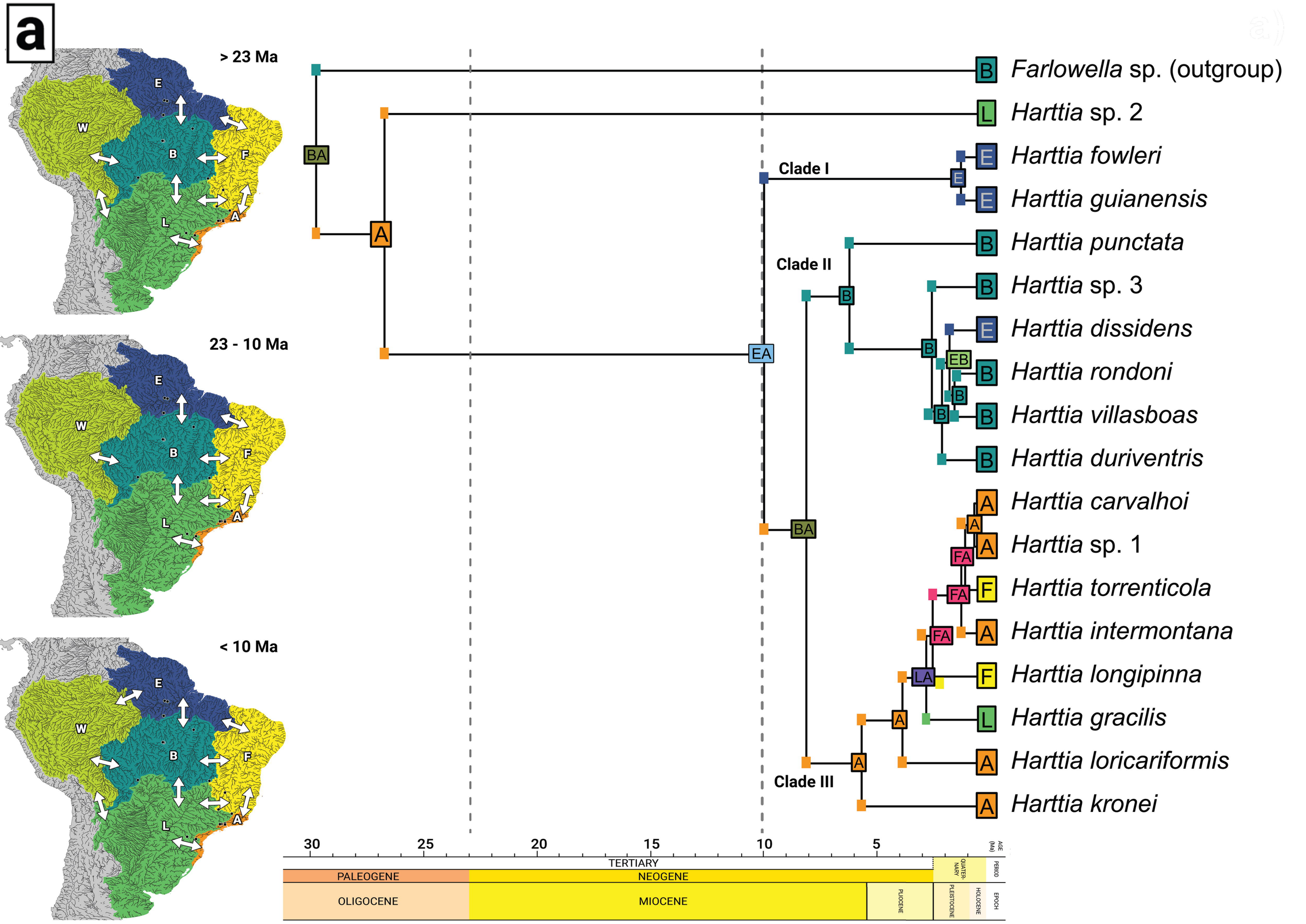
a
> 23 Ma
23 - 10 Ma
< 10 Ma
E
W
B
F
L
A
BA
EA
LA
FA
Clade I
Clade II
Clade III
Farlowella sp. (outgroup)
Harttia sp. 2
Harttia fowleri
Harttia guianensis
Harttia punctata
Harttia sp. 3
Harttia dissidens
Harttia rondoni
Harttia villasboas
Harttia duriventris
Harttia carvalhoi
Harttia sp. 1
Harttia torrenticola
Harttia intermontana
Harttia longipinna
Harttia gracilis
Harttia loricariformis
Harttia kronei
30
25
20
15
10
5
AGE (Ma)
TERTIARY
PALEOGENE
NEOGENE
QUATERNARY
PERIOD
OLIGOCENE
MIOCENE
PLIOCENE
PLEISTOCENE
HOLOCENE
EPOCH

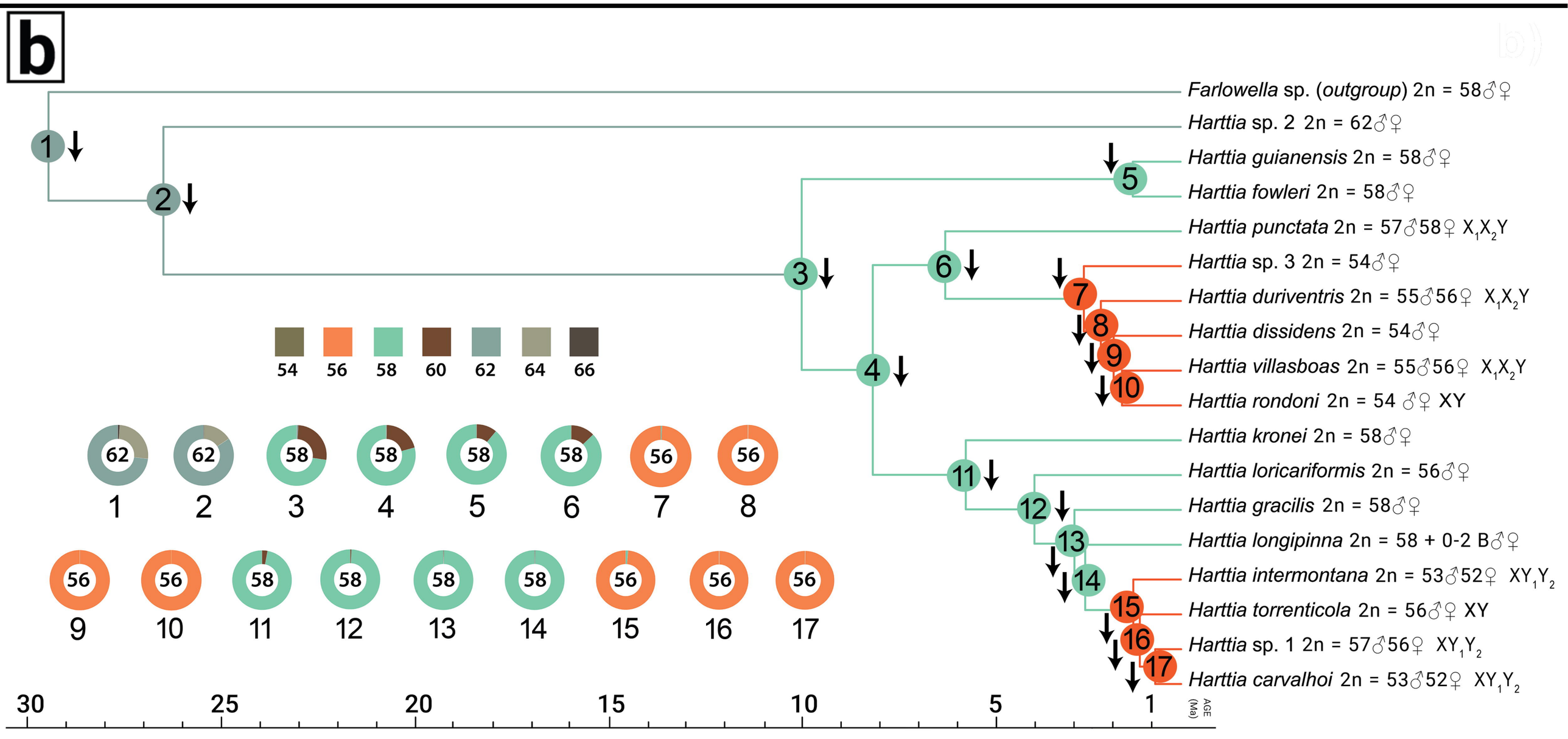
b
Farlowella sp. (outgroup) 2n = 58♂♀
Harttia sp. 2 2n = 62♂♀
Harttia guianensis 2n = 58♂♀
Harttia fowleri 2n = 58♂♀
Harttia punctata 2n = 57♂58♀ X1X2Y
Harttia sp. 3 2n = 54♂♀
Harttia duriventris 2n = 55♂56♀ X1X2Y
Harttia dissidens 2n = 54♂♀
Harttia villasboas 2n = 55♂56♀ X1X2Y
Harttia rondoni 2n = 54 ♂♀ XY
Harttia kronei 2n = 58♂♀
Harttia loricariformis 2n = 56♂♀
Harttia gracilis 2n = 58♂♀
Harttia longipinna 2n = 58 + 0-2 B♂♀
Harttia intermontana 2n = 53♂52♀ XY1Y2
Harttia torrenticola 2n = 56♂♀ XY
Harttia sp. 1 2n = 57♂56♀ XY1Y2
Harttia carvalhoi 2n = 53♂52♀ XY1Y2
54
56
58
60
62
64
66
30
25
20
15
10
5
1
AGE (Ma)

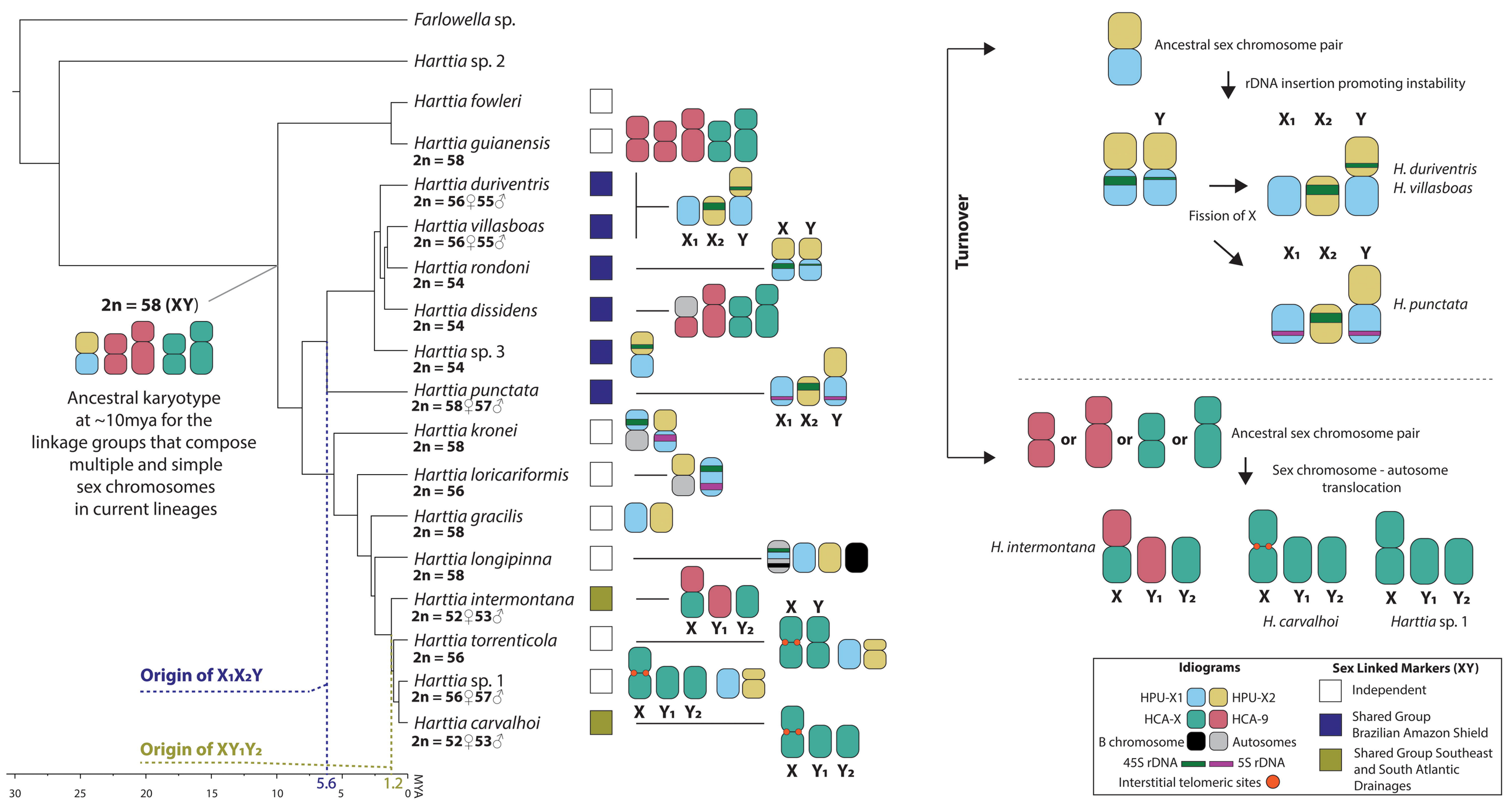
Farlowella sp.
Harttia sp. 2
Harttia fowleri
Harttia guianensis
2n = 58
Harttia duriventris
2n = 56♀55♂
Harttia villasboas
2n = 56♀55♂
Harttia rondoni
2n = 54
Harttia dissidens
2n = 54
Harttia sp. 3
2n = 54
Harttia punctata
2n = 58♀57♂
Harttia kronei
2n = 58
Harttia loricariformis
2n = 56
Harttia gracilis
2n = 58
Harttia longipinna
2n = 58
Harttia intermontana
2n = 52♀53♂
Harttia torrenticola
2n = 56
Harttia sp. 1
2n = 56♀57♂
Harttia carvalhoi
2n = 52♀53♂
2n = 58 (XY)
Ancestral karyotype at ~10mya for the linkage groups that compose multiple and simple sex chromosomes in current lineages
Origin of X1X2Y
Origin of XY1Y2
30
25
20
15
10
5
0
MYA
5.6
1.2
X1 X2 Y
X Y
X1 X2 Y
X Y1 Y2
X Y
X Y1 Y2
X Y1 Y2
Turnover
Ancestral sex chromosome pair
rDNA insertion promoting instability
Y
X1 X2 Y
H. duriventris
H. villasboas
Fission of X
X1 X2 Y
H. punctata
or
or
or
Ancestral sex chromosome pair
Sex chromosome - autosome translocation
H. intermontana
X Y1 Y2
X Y1 Y2
H. carvalhoi
X Y1 Y2
Harttia sp. 1
Idiograms
HPU-X1
HPU-X2
HCA-X
HCA-9
B chromosome
Autosomes
45S rDNA
5S rDNA
Interstitial telomeric sites
Sex Linked Markers (XY)
Independent
Shared Group Brazilian Amazon Shield
Shared Group Southeast and South Atlantic Drainages